

AD-A087 608

TEL-AVIV UNIV (ISRAEL) DEPT OF GEOPHYSICS AND PLANET--ETC F/G 4/1
SIZE DISTRIBUTION, CHEMICAL COMPOSITION AND OPTICAL PROPERTIES --ETC(U)
FEB 80 Z LEVIN

DA-ERO-78-6-087

NL

UNCLASSIFIED

1 1 1

2 1 1

3 1 1

4 1 1

5 1 1

6 1 1

7 1 1

8 1 1

9 1 1

10 1 1

11 1 1

12 1 1

13 1 1

14 1 1

15 1 1

16 1 1

17 1 1

18 1 1

19 1 1

20 1 1

21 1 1

22 1 1

23 1 1

24 1 1

25 1 1

26 1 1

27 1 1

28 1 1

29 1 1

30 1 1

31 1 1

32 1 1

33 1 1

34 1 1

35 1 1

36 1 1

37 1 1

38 1 1

39 1 1

40 1 1

41 1 1

42 1 1

43 1 1

44 1 1

45 1 1

46 1 1

47 1 1

48 1 1

49 1 1

50 1 1

51 1 1

52 1 1

53 1 1

54 1 1

55 1 1

56 1 1

57 1 1

58 1 1

59 1 1

60 1 1

61 1 1

62 1 1

63 1 1

64 1 1

65 1 1

66 1 1

67 1 1

68 1 1

69 1 1

70 1 1

71 1 1

72 1 1

73 1 1

74 1 1

75 1 1

76 1 1

77 1 1

78 1 1

79 1 1

80 1 1

81 1 1

82 1 1

83 1 1

84 1 1

85 1 1

86 1 1

87 1 1

88 1 1

89 1 1

90 1 1

91 1 1

92 1 1

93 1 1

94 1 1

95 1 1

96 1 1

97 1 1

98 1 1

99 1 1

100 1 1

END

DATE

FILED

9 80

DTIC

LEVEL II

AD

(12)

SIZE DISTRIBUTION, CHEMICAL COMPOSITION AND OPTICAL PROPERTIES
OF ATMOSPHERIC DUST IN ISRAEL: A COMPARISON OF URBAN AND
DESERT AEROSOLS UNDER CLEAR AND DUSTY CONDITIONS

Final Technical Report

by

Zev Levin

February 1980

European Research Office
United States Army
London N.W.I, England

Grant No. DA-ERO-78-G-087

DTIC
ELECTE
AUG 04 1980
S D E

Department of Geophysics and Planetary Sciences
Tel Aviv University
Ramat Aviv, Israel.

Approved for public release: distribution unlimited

ADA 087608

DDC FILE COPY

80 7 29 034

REPORT DOCUMENTATION PAGE		READ INSTRUCTIONS BEFORE COMPLETING FORM
1. Report Number	2. Govt Accession No. AD-A087608	3. Recipient's Catalog Number
4. Title (and Subtitle) Size Distribution, Chemical Composition and Optical Properties of Atmospheric Dust in Israel: A Comparison of Urban and Desert Aerosols under Clear and Dusty Conditions		5. Type of Report & Period Covered Final Report 1 July 1978 - 1 March 1980
7. Author(s) Zev/Levin		8. Contract or Grant Number DA-ERO-78-G-087
9. Performing Organization Name and Address Department of Geophysics and Planetary Sciences, Tel Aviv University, Ramat Aviv, Israel		10. Program Element, Project, Task Area & Work Unit Numbers 1273
11. Controlling Office Name and Address U.S. Army R & S Group (EUR), P.O. Box 65.		12. Report Date February 1980
14. Monitoring Agency Name and Address		13. Number of Pages 71
		15. Security Class (of this report) Unclassified
16. & 17. Distribution Statement Approved for public release; distribution unlimited.		
18. Supplementary Notes		
19. Key Words (1) Atmospheric Aerosols; (2) Dust; (3) Size Distribution; (4) Chemical Composition; (5) Optical Properties; (6) Remote Sensing.		
20. Abstract <p>Measurements of aerosol size distributions, chemical composition and optical properties were carried out at two locations in Israel. Tel Aviv was chosen as an urban region and Mitzpe Ramon as a desert region. The measurements indicate that the size spectra between 0.15 - 12 μm can be approximated by a power law type distribution. The spectra in Tel Aviv show higher concentrations and greater slopes than those from the desert. Diurnal variations between day and night are observed in the size distribution of the summertime measurements in Tel Aviv. These are believed to be related to the increase in aerosol size due to absorption of water.</p>		

SECURITY CLASSIFICATION OF THIS PAGE: UNCLASSIFIED
vapor during high relative humidity periods. The chemical composition in Tel Aviv was found to strongly depend on the meteorological conditions.

The optical measurements also suggest strong differences between Tel Aviv and the desert. Filter samples of atmospheric particulate matter from Tel Aviv always appeared darker than those from the desert site. Measurements of imaginary refractive index in the 0.3 to 1.7 μm spectral region are presented. These measurements are consistently higher by a factor of 2 to 4 in Tel Aviv as compared to simultaneous samples from the desert site. Seasonal variations have also been observed and are believed to be primarily related to temperature inversions near or at the ground during the winter months and to the effect of pollution from Southern Europe which is carried eastward by synoptic scale motion.

The size distribution, composition and imaginary refractive index observations are interpreted in terms of aerosol origins and prevailing local and synoptic scale meteorological conditions.

In addition, some simultaneous measurements of optical depth and size distribution in a dust storm are presented. The measured and derived properties of the aerosol are compared with each other and with other results published in the scientific literature. We observe some global commonality in the measured size spectra of desert aerosols especially for post-frontal conditions. On the other hand, during the passage of the front itself, high aerosol concentrations with a sharp peak in radius at about 1 μm were observed. These were not generally similar to other size distributions reported in the literature.

The imaginary part of the refractive index in the spectral region (0.3 - 1.7 μm) was found to be similar to that found in other deserts. Comparison of the optical measurements with the direct sampling data suggests that the general time trends of the size distributions as measured in-situ, are followed by the optical depth and its variations with wavelength. On the other hand, detailed short-term fluctuations detected by our direct measurements are not followed by the optical method. We have observed that a simple power law for the size distribution is a reasonable approximation only during clear and calm conditions with small optical depth. During the dust storm itself, the deviations from a power law are large as shown by both direct in-situ and optical observations.

Unclassified

SECURITY CLASSIFICATION OF THIS PAGE: UNCLASSIFIED

Table of Contents

	Page
Abstract	1
Preface	3
Part I: Size distribution, chemical composition and optical properties of urban and desert aerosols in Israel.	4
a. Introduction	4
b. The Measuring Sites	4
c. Aerosols Size Distribution	6
Winter-time measurements	8
Summer-time measurements	12
d. Optical Properties and Composition	16
e. Summary of Observations	33
f. Conclusion	34
Part II: Properties of Sharav (Khamsin) Dust - Comparison of Optical and Direct Sampling Data	36
a. Introduction	36
b. The Data Acquisition System	38
c. Data and Analysis	40
i. Size Distribution	40
ii. Imaginary Refractive Index	47
iii Spectral Transmission of the Atmosphere	47
d. Summary and Conclusions	59
Acknowledgements	60
References	61

Accession For	
NTIS GRA&I	<input checked="checked" type="checkbox"/>
DDC TAB	<input type="checkbox"/>
Unannounced	<input type="checkbox"/>
Justification	
By _____	
Distribution/ _____	
Availability Codes	
Dist. A	Avail and/or special

List of Figures and Tables

- Fig. 1 A map of Israel showing the measuring sites.
- Fig. 2 Typical size distributions of aerosol particles from both Tel Aviv and Mitzpe Ramon, during the day and night, in comparison with measurements of Patterson and Gillette (1977) at Haswell, Colorado.
- Fig. 3 Variations with time of the size distribution and aerosol particle concentrations during two winter periods in Tel Aviv. β is the exponent and C is the proportionality constant in Eq. (1). N is the number concentration in no./cm³.
- Fig. 4 Variation with time of the size distribution and aerosol particle concentrations during a winter period in Mitzpe Ramon. Negev desert.
- Fig. 5 Comparison of normalized frequency distributions of β for Tel Aviv and Mitzpe Ramon from winter observations. (a) Daytime and (b) night-time measurements.
- Fig. 6 Typical variations with time of the size distribution and aerosol particle concentrations during two summer periods in Tel Aviv.
- Fig. 7 Variation of aerosol particle concentration, relative humidity and wind direction for the two sampling periods shown in Fig. 6.
- Fig. 8 Membrane filter samples of atmospheric dust from Israel. The upper two samples are from Mitzpe Ramon in the Negev desert. The bottom three are from Tel Aviv. The lighter of the three Tel Aviv samples (the one on the lower right hand side), shows the influence of persistent easterly wind conditions contributing additional desert dust to the normally dark appearing urban sample.

- Fig. 9 Infrared potassium bromide disk transmission spectra of several atmospheric dust samples from Israel. These examples were chosen to show the kind of variability that occurs. The letters indicate the substances that can account for individual absorption features. Note the high degree of variability in the 8 to 14 μm spectral region.
- Fig. 10a Electron micrographs of typical aerosol particles observed in Tel Aviv during westerly flow conditions (Sept. 1976). The elemental composition was obtained by an electron microprobe.
- Fig. 10b The same as Fig. 10a except during easterly flow conditions on February 4, 1977.
- Fig. 11 Typical examples of the imaginary refractive index spectra for two atmospheric dust samples from Israel compared to several samples from other localities. In general, samples from urban areas such as Tel Aviv and the three European sites shown show much higher imaginary indices than do those from the Negev desert or the two American desert localities (Lindberg et al., 1976).
- Fig. 12 Imaginary refractive index values at 0.7 μm wavelength, for all of the atmospheric dust samples. The horizontal lines indicate the time interval on the abscissa during which the individual sample was collected. Note that in all cases those from Tel Aviv are much higher than values obtained nearly simultaneously from the Negev desert. There is also a clear increase in measured values during the winter months. The curve represents 3 months averages and the bars the standard deviation. The data points with squares were deleted from the averages since they represent samples which were strongly affected by dust from the desert during easterly flow in Tel Aviv.

- Fig. 13 Synoptic maps of the Weather Situation on 6 June, 1977,
(a) 8:00 LST and (b) 14:00 LST.
- Fig. 14 The Normal-Incidence Sun-Following Automatic Interference
Filter Spectrophotometer.
- Fig. 15 Time variations of the total number concentration in the size
range 0.15 - 12.5 μm .
- Fig. 16 Size distribution, $\frac{dN}{d\log r}$, of desert aerosol measured at surface
level at Mitzpe Ramon, 6-7-8 June 1977 with a Royco 220.
- Fig. 17 Volume distributions, $\frac{dV}{d\log r}$ under conditions of Fig. 16.
- Fig. 18 Area distributions $\frac{dS}{d\log r}$, under conditions of Fig. 16.
- Fig. 19 The imaginary part of the refractive index in the solar spectral
range during the period of the storm.
- Fig. 20 The total mean number-density, N , the optical depth at wavelength
0.45 μm , τ_1 (a): the constant C of the average power-law size
distribution ($\frac{dN}{d\log r} = Cr^{-\beta}$), (b); the constant A of the average
wavelength dependence of the optical depth ($\tau(\lambda) = \tau_1 A(\frac{\lambda}{0.45})^{-\beta}$)
(c); the average slope of the size distribution, β , derived from
in-situ (Royco) and optical data (d).

- Fig. 21 The optical depths, $\tau(0.45 \mu\text{m})$ and $\tau(0.65 \mu\text{m})$ and the wavelength exponent α , versus time.
- Fig. 22 Typical curves of optical depth versus wavelength during the storm compared to data from other locations and from other times at Mitzpe Ramon, (S.A.L stands for Saharan Aerosol Layer).
- Table 1 Average values and standard deviations of the parameters from Eq. 1 for both winter and summer measurements at Mitzpe Ramon and Tel Aviv.
- Table 2 X-ray count ratio of different elements to Si.
- Table 3 Properties of aerosols on June 6-8, 1977
 (a) Fit to power-law size distribution $\frac{dn}{d\log r} = Cr^{-\beta}$
 (b) The optical depth of dust on 6/6/77.

Accession For	
NTIS GRA&I	<input checked="" type="checkbox"/>
DDC TAB	<input checked="" type="checkbox"/>
Unannounced	<input type="checkbox"/>
Justification	
By	
Distribution/	
Availability Codes	
Available/only	
Dist. Special	

Abstract

Measurements of aerosol size distributions, chemical composition and optical properties were carried out at two locations in Israel. Tel Aviv was chosen as an urban region and Mitzpe Ramon as a desert region. The measurements indicate that the size spectra between $0.15 - 12 \mu\text{m}$ can be approximated by a power-law type distribution. The spectra in Tel Aviv show higher concentrations and greater slopes than those from the desert. Diurnal variations between day and night are observed in the size distribution of the summertime measurements in Tel Aviv. These are believed to be related to the increase in aerosol size due to absorption of water vapor during high relative humidity periods. The chemical composition in Tel Aviv was found to strongly depend on the meteorological conditions.

The optical measurements also suggest strong differences between Tel Aviv and the desert. Filter samples of atmospheric particulate matter from Tel Aviv always appeared darker than those from the desert site. Measurements of imaginary refractive index in the 0.3 to $1.7 \mu\text{m}$ spectral region are presented. These measurements are consistently higher by a factor of 2 to 4 in Tel Aviv as compared to simultaneous samples from the desert site. Seasonal variations have also been observed and are believed to be primarily related to temperature inversions near or at the ground during the winter months and to the effect of pollution from Southern Europe which is carried eastward by synoptic scale motion.

The size distribution, composition and imaginary refractive index observations are interpreted in terms of aerosol origins and prevailing local and synoptic scale meteorological conditions.

In addition, some simultaneous measurements of optical depth and size distribution in a dust storm are presented. The measured and derived properties of the aerosol are compared with each other and with other results published in the scientific literature. We observe some global commonality in the measured size spectra of desert aerosols especially for post frontal conditions. On the other hand, during the passage of the front itself, high aerosol concentrations with a sharp peak in radius at about $1 \mu\text{m}$ were observed. These were not generally similar to other size distributions reported in the literature.

The imaginary part of the refractive index in the spectral region (0.3 - 1.7 μm) was found to be similar to that found in other deserts. Comparison of the optical measurements with the direct sampling data suggests that the general time trends of the size distributions as measured in-situ, are followed by the optical depth and its variations with wavelength. On the other hand, detailed short-term fluctuations detected by our direct measurements are not followed by the optical method. We have observed that a simple power law for the size distribution is a reasonable approximation only during clear and calm conditions with small optical depth. During the dust storm itself, the deviations from a power-law are large as shown by both direct in-situ and optical observations.

PREFACE

This report summarizes work that was carried out over the past four years in Israel. Measurements of aerosol properties both in an urban and desert environment were carried out almost continuously over this period. During that time a few special experiments were conducted in order to be able to characterize the aerosols under specific meteorological conditions.

This report is therefore divided into two parts: (I) A general look at the aerosol in the Eastern Mediterranean through a comparison of the physical chemical and optical properties of the atmospheric aerosols in an urban and desert environment. (II) A specific study of Sharav (Khamsin) dust with a comparison of results between optical and direct sampling methods.

Part 1: Size Distribution Chemical Composition and Optical Properties
of Urban and Desert Aerosols in Israel.

a. Introduction

Much attention has been recently devoted to the influence of atmospheric aerosols on the atmospheric radiation budget and its long-term effects on climate. Changes in the amounts and composition of atmospheric particulates can strongly influence surface temperature and as a result change the atmospheric stability and modify the general circulation patterns (e.g. SMIC 1971).

Atmospheric aerosols can be divided into natural and anthropogenic types. The most widespread natural aerosols are those originating from deserts while sources of anthropogenic aerosols could be identified as major urban areas. The effect of these aerosols on the local and global climate are through their effects on the albedo, absorption and scattering of radiation. These processes are strongly affected by the optical properties of the aerosols, by the number concentration and their size distribution.

In this part of the report, we would like to describe some results of measurements of these parameters in a desert region in Israel and compare them to measurements in an urban area (Tel Aviv). Some of these results will then be compared with other measurements taken in other parts of the world.

b. The Measuring Sites

Two measuring sites were established in Israel: (1) at the Tel Aviv University campus, located at the north end of the city of Tel Aviv (see fig. 1). The aerosol measuring instruments were mounted on the top of the building of the Department of Geophysics and Planetary Sciences at about 20 m above ground. 40 meters above sea level and about 1 km from the sea shore. (2) The second site was established at Mitzpe Ramon, in the middle of the Negev desert (see Fig. 1). The instruments were mounted on the top of the Astronomical Observatory of Tel Aviv University (about 8 m above ground) located at about 900 m above sea level.

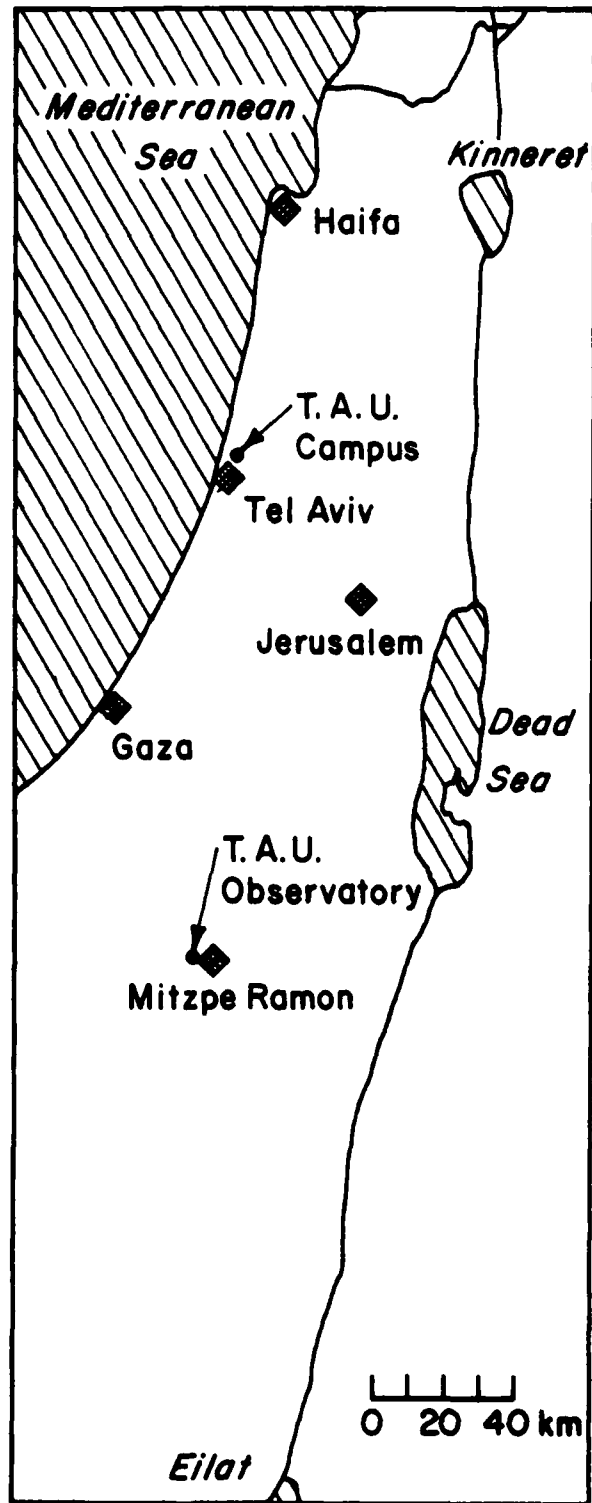


Fig. 1. A map of Israel showing the measuring sites.

c. Aerosols Size Distribution

The measurements of the size distributions of the aerosols in both Mitzpe Ramon (Negev desert) and in Tel Aviv, Israel, were carried out by the use of a well-calibrated aerosol optical counter (Royco 220). The instrument was calibrated with dry Latex particles of known sizes which were dispersed from a liquid suspension by the use of an ultrasonic nebulizer (Devilbis). The optical counter categorized the aerosols into six size classes: 0.15-0.32, 0.32-0.75, 0.75-1.5, 1.5-3, 3-7.5, and >7.5 μm based on the amount of light scattered at 90° into a photomultiplier tube.

The instrument was set to record 4 samples of one minute each during every 15 minutes. The data presented here therefore, represents averages of 4 size spectra every 15 minutes. Measurements of size distribution were carried out at both sites during the winter and early spring of 1976. Measurements in Tel Aviv continued into the summer months as well.

Figure 2 presents examples of distributions of atmospheric aerosols both in Tel Aviv and Mitzpe Ramon for both day and night measurements. The summer time night measurements in Tel Aviv usually showed higher aerosol concentration than during the day. This point will be discussed further later on. In Fig. 2 we also plotted the "typical" soil derived aerosol size distribution measured by Patterson and Gillette (1977) in Colorado. We see that our measurements for the desert fall mostly below theirs. On the other hand, Tel Aviv night-time spectra was higher. We can also see the appearance of a small peak in our measurements around 1-1.2 μm . The slopes of all our measurements are smaller than that observed by Patterson and Gillette (1977).

Since in this study we are concerned with time variations of the aerosol size spectra, we need to find a function whose parameters' variations with time could be easily presented. From Fig. 2 we see that the distribution can probably be fitted with a combination of a few log-normal distributions. However we felt that for the purpose of presenting the time variations of the size spectra a Junge-type distribution would be the simplest, being fully aware that in presenting the data this way we lose some information. A best fit to the data based on the equation

$$\frac{dN}{d\log r} = C r^{-\beta} \quad (1)$$

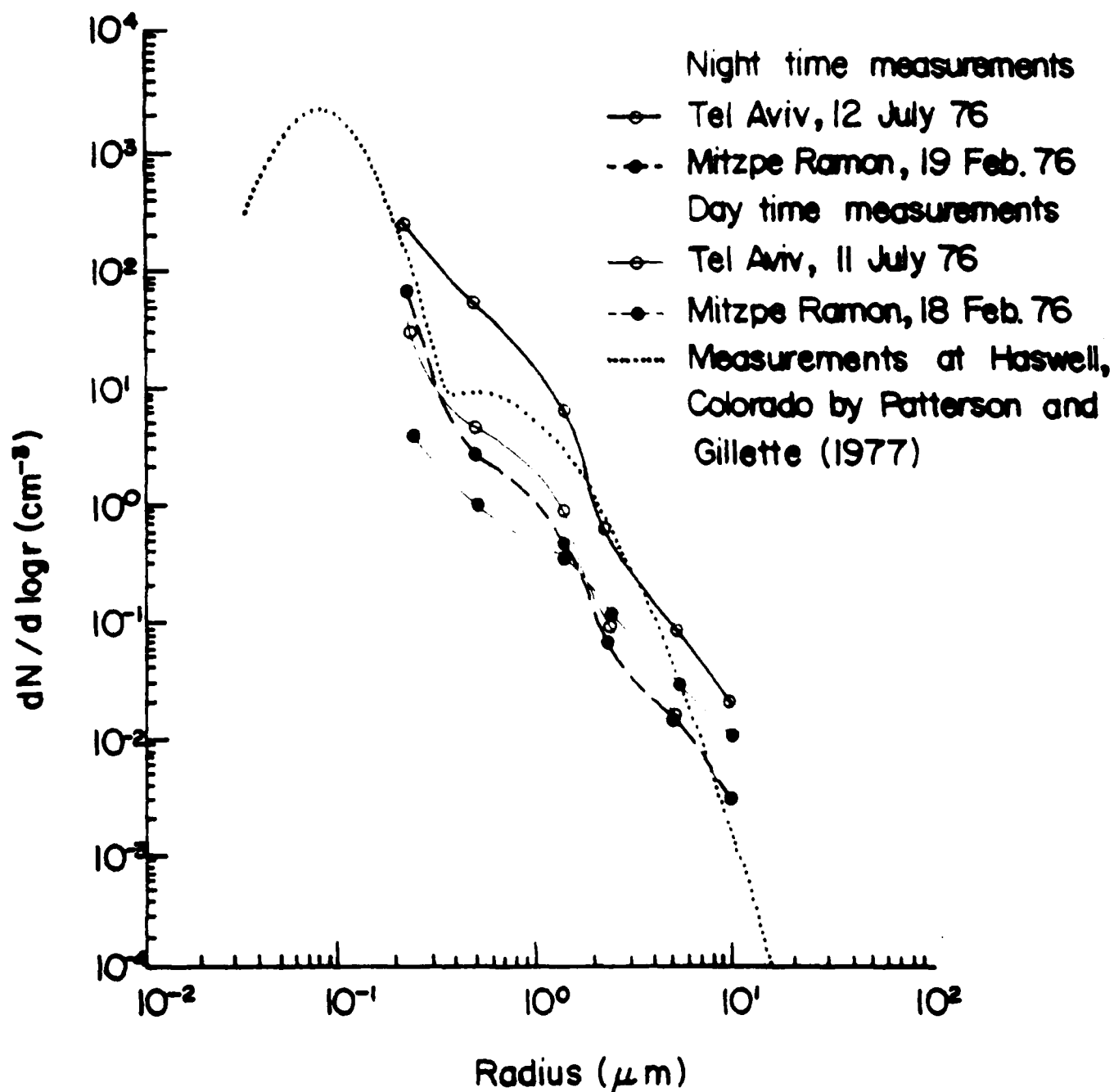


Fig. 2 Typical size distributions of aerosol particles from both Tel Aviv and Mitzpe Ramon, during the day and night, in comparison with measurements of Patterson and Gillette (1977) at Haswell, Colorado.

was obtained for every set of 4 one minute measurements. The average value of C , β and N (the total number concentration of the aerosols) were then recorded as a function of time (see Figs. 3 and 4).

Winter-time measurements.

Figures 3a and b represent the variations of β and C during two periods in March 1976 in Tel Aviv while Fig. 4 represents these parameters from measurements in Mitzpe Ramon. On the same graphs the concentrations of aerosol particles in no./cm^3 (with $r > 0.15 \mu\text{m}$) are plotted as a function of time. Many of the winter day-time measurements taken at Tel Aviv generally showed higher concentration of particles, due to local pollution. The Tel Aviv winter night measurements indicate a reduction in the total aerosol content. The day-time values of β in Tel Aviv vary between about 1.4 and 3.0 while in the desert they vary between 1.2 and 2.8. The relatively large values of β in Tel Aviv indicate the presence of a large number of small particles. This is more easily seen when we look at Fig. 5a, which represents a frequency distribution of β for both day and night measurements in Tel Aviv and the desert.

We see that on the average the β values encountered in the Negev are lower which suggests the presence of proportionately higher number of large particles. This is an expected result, since locally generated aerosols in the desert tend to be soil aerosols which are larger than about $1 \mu\text{m}$ (e.g. Patterson and Gillette, 1977). On the other hand, aerosols generated in urban areas tend to start off smaller since they are mostly generated by gas-to particle conversion. Comparison of the β values from Tel Aviv between day and night (Fig. 5a and b) reveals a decrease in the average value of β at night. This may suggest either a decrease of the small particle concentration or an increase in concentration of the larger particles relative to the small ones.

The frequency distribution of β for the winter night-time measurements in Mitzpe Ramon suggest slightly larger β values than those measured in Tel Aviv. Unfortunately, this distribution is only based on relatively few measurements and no definite conclusion can be drawn from it. Of course, as expected, the number concentration of the aerosols in the urban area is considerably higher than that number in a desert environment.

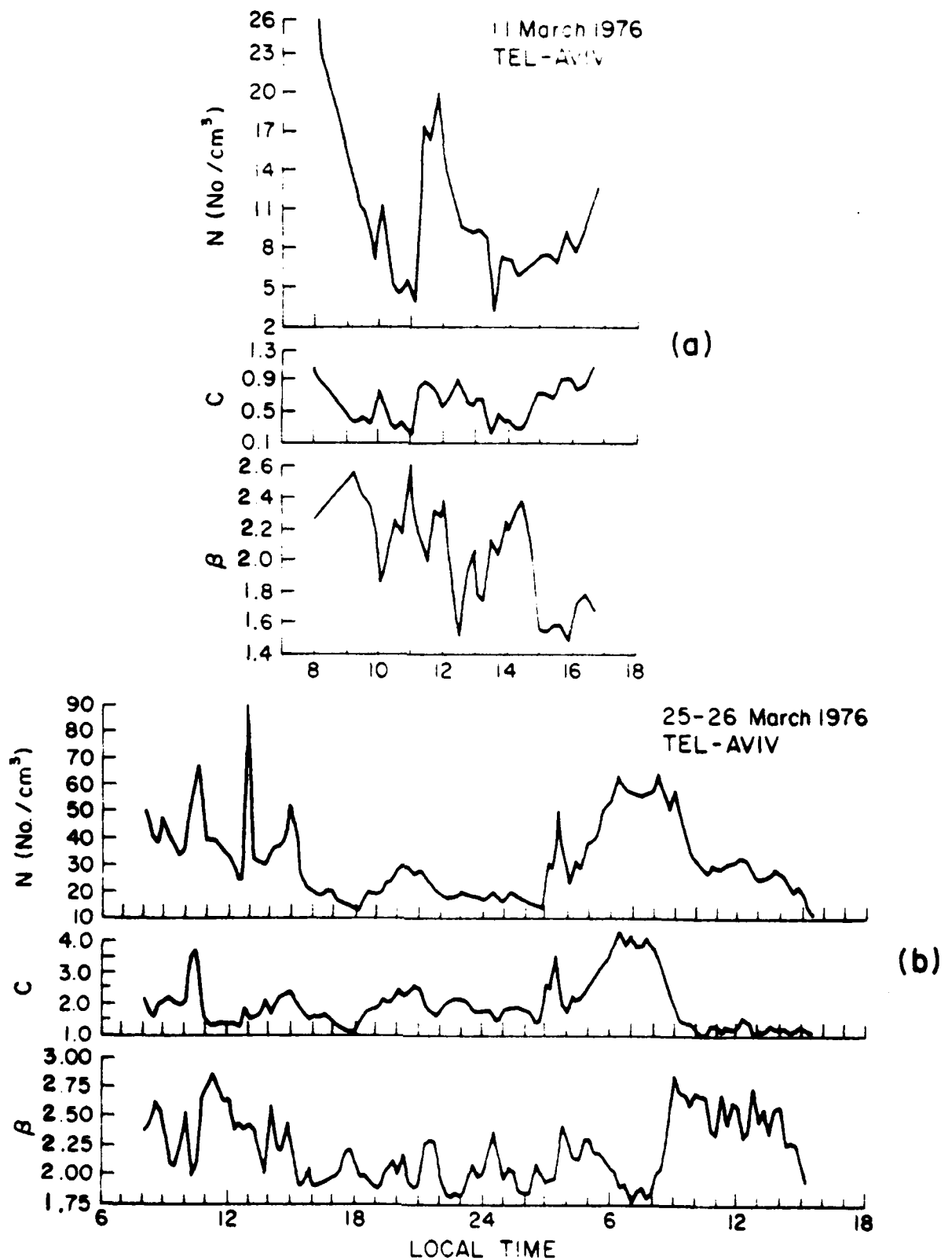


Fig. 3 Variations with time of the size distribution and aerosol particle concentrations during two winter periods in Tel Aviv. β is the exponent and C is the proportionality constant in Eq. (1). N is the number concentration in no./cm³.

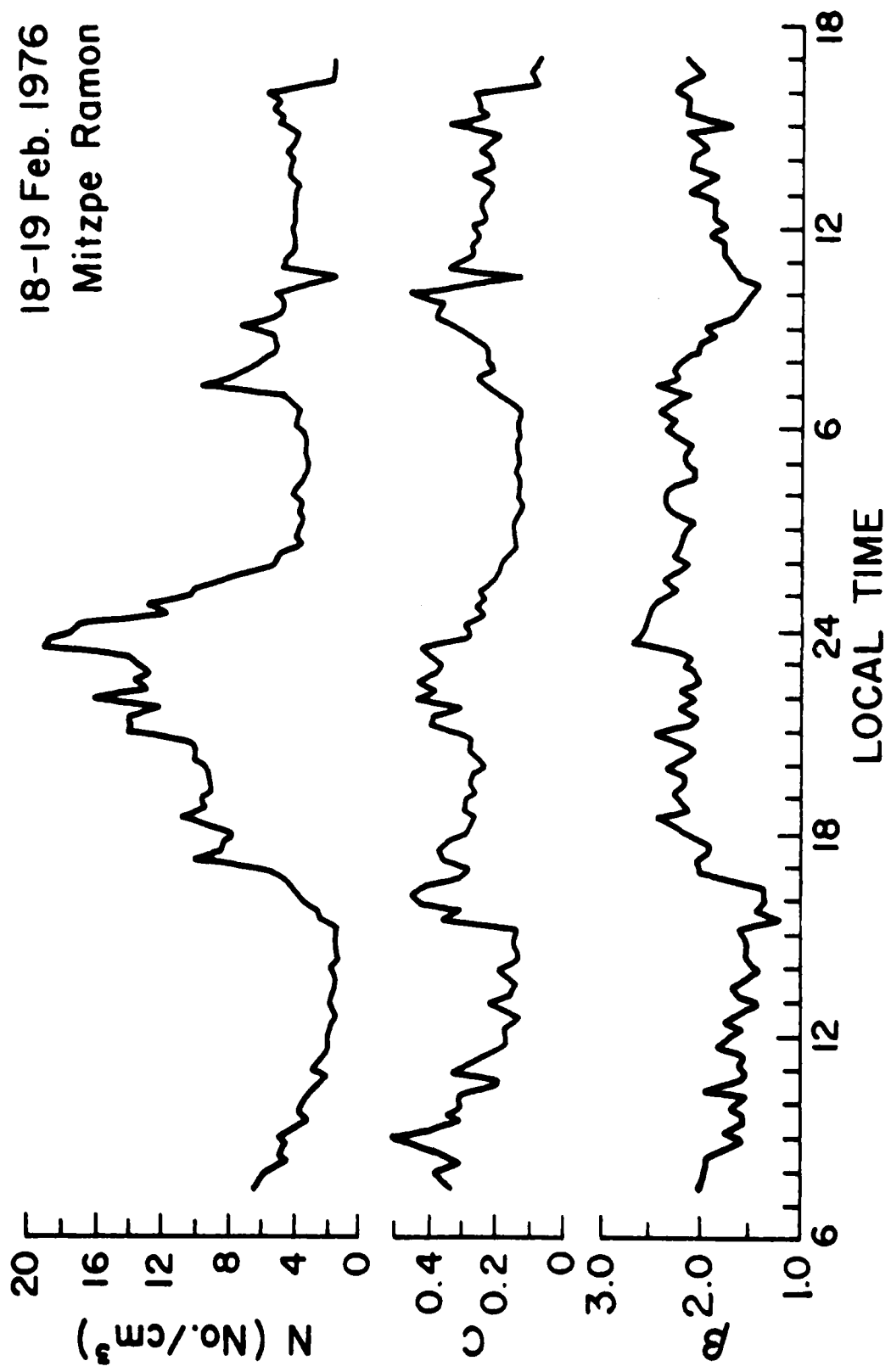


Fig. 4 Variation with time of the size distribution and aerosol particle concentrations during a winter period in Mitzpe Ramon, Negev desert.

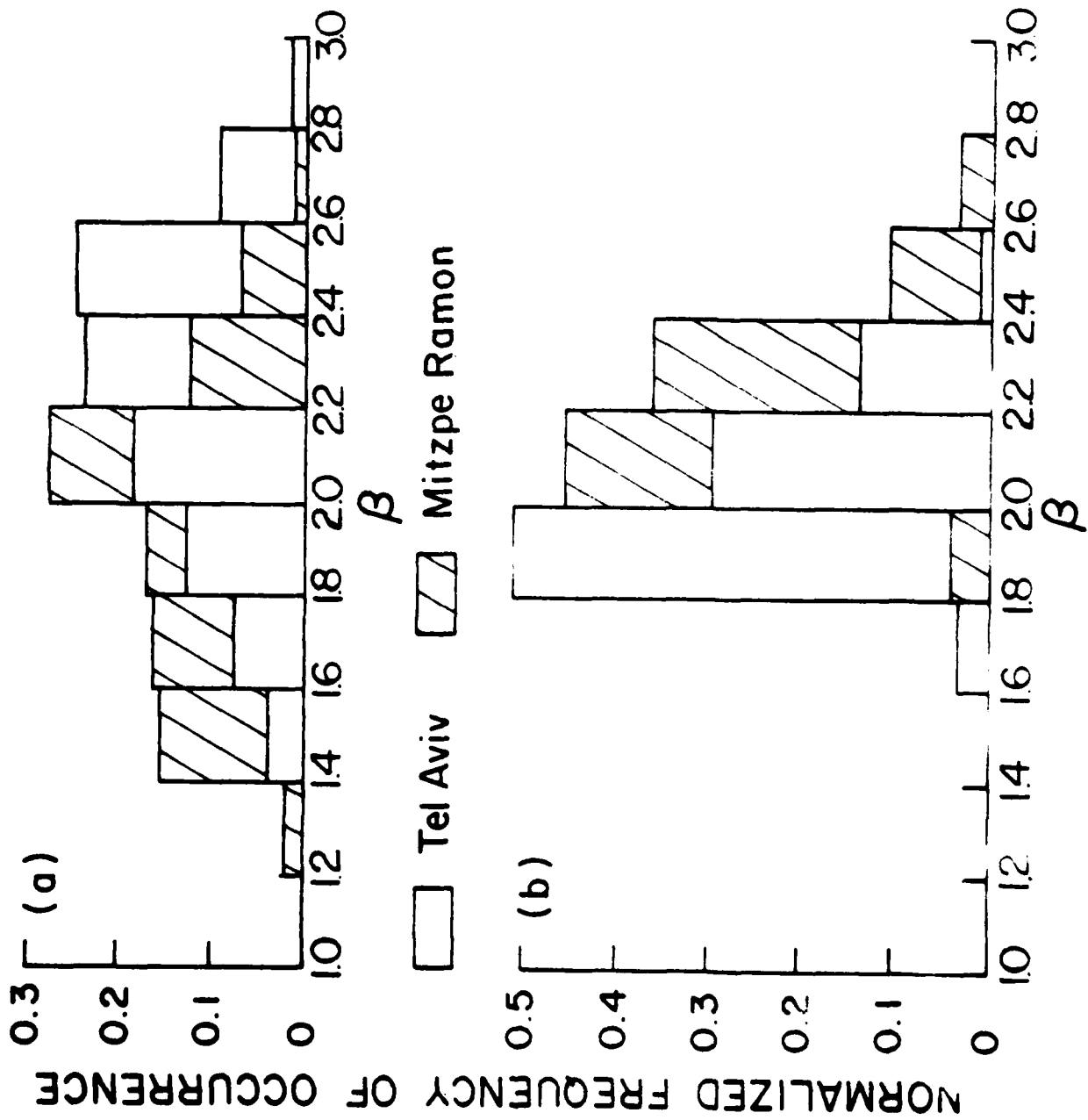


Fig. 5 Comparison of normalized frequency distributions of β for Tel Aviv and Mitzpe Ramon from winter observations. (a) Daytime and (b) night-time measurements.

Table 1 presents average values and standard deviations of atmospheric aerosols ($r > 0.15 \mu\text{m}$) under winter conditions at Mitzpe Ramon and Tel Aviv.

Summertime measurements.

The summer measurements were carried out in Tel Aviv only. They were carried out almost continuously from the beginning of July to the middle of September 1976. A few typical variations are presented in Figs. 6a and b. One striking feature that can be seen is the increase in particle concentration around midnight in almost all our summertime measurements. Somewhat similar increase is also seen at night in the winter data from Mitzpe Ramon (see Fig. 4).

There could be a few possible reasons for this increase: (1) A shift in the wind direction which advects large concentrations of aerosol from the city to the sampling site. (2) A swelling of the particles as a result of an increase in the ambient relative humidity (Hanel 1976). (3) A decrease in the height of the mixing layer and therefore a reduction in the dilution of the atmospheric aerosols. The first reason was believed to have only a second order effect in this case. This is because very often the increase in the number concentration was observed to occur before the wind shifted direction. For example, Figs. 7a and b suggest that on July 11-12 and September 2-3, the wind brought polluted air to the sampling site only 1 and 1.5 hours respectively after the increase in the concentration was observed.

A somewhat better correlation was observed between the increase in relative humidity above about 75% and the increase in the total number concentrations (see Fig. 7 for Sept. 2-3). This increase can be explained by the absorption of water vapor by the hygroscopic component of the aerosols as was shown theoretically by Hanel (1976) and experimentally by Gillette (private communication). This implied that all the particles in the size distribution grow in size so that particles that otherwise would be smaller than the detection threshold of the instrument grow to sizes that can be recorded. Hanel (1976) showed that the increase in radius could be over 20% when the relative humidity exceeds 80%. This increase in size is a relatively weak function of the initial size of the particles, which implies that the whole size distribution shifts along the radius axis and only minor variations in β should occur. Of course, changes in size depend on the chemical nature of the

Location	Season	period over which average is taken	C	β
Mitzpe Ramon	Winter	24 hr	0.21 ± 0.1	2 ± 0.3
Tel Aviv	Winter	daytime	1.2 ± 0.86	2.2 ± 0.3
Tel Aviv	Winter	night-time	1.92 ± 0.46	2.04 ± 0.16
Tel Aviv	Summer	daytime	0.56 ± 0.16	2.39 ± 0.19
Tel Aviv	Summer	night-time	1.1 ± 0.3	2.35 ± 0.18
Tel Aviv	Summer	24 hr	0.91 ± 0.14	2.36 ± 0.19

Table 1.

Average values and standard deviations of the parameters from Eq. 1 for both winter and summer measurements at Mitzpe Ramon and Tel Aviv.

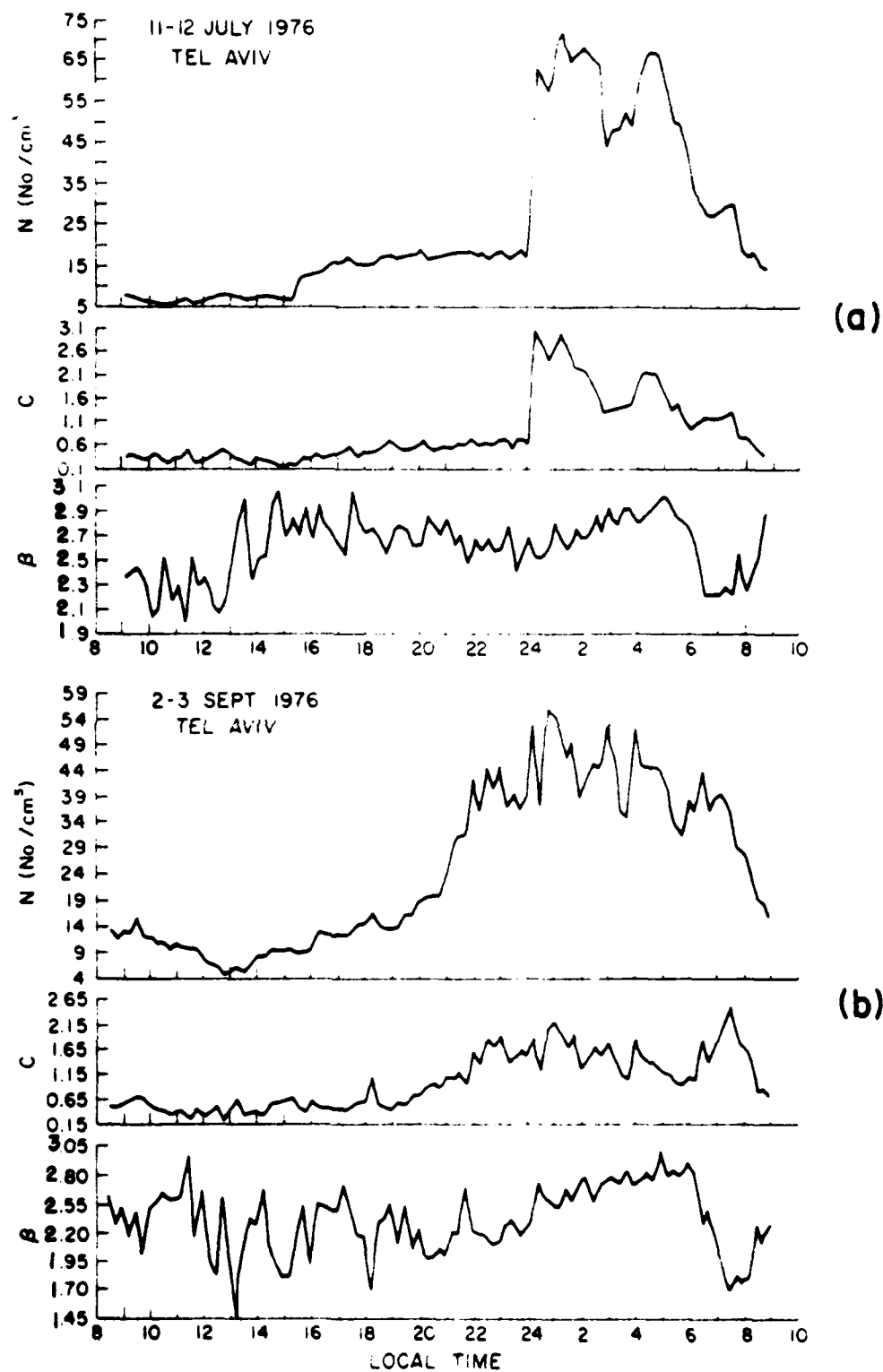


Fig. 6 Typical variations with time of the size distribution and aerosol particle concentrations during two summer periods in Tel Aviv.

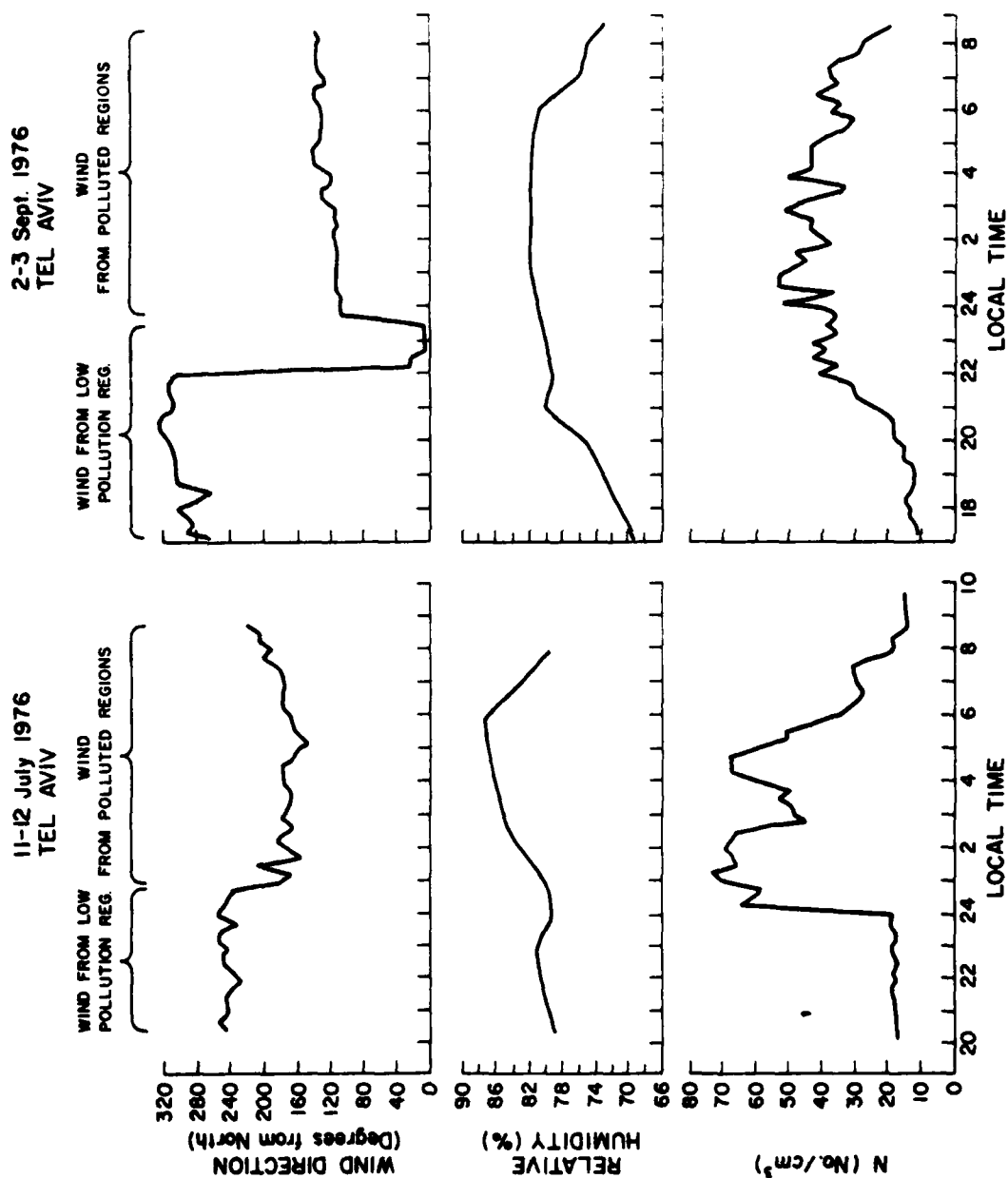


Fig. 7 Variation of aerosol particle concentration, relative humidity and wind direction for the two sampling periods shown in Fig. 6.

particles. We would expect hygroscopic particles to rapidly grow in size with increasing humidity, while only small increases in size for non-hygroscopic particles should occur under similar conditions. During the periods of increase in N some small variations in β are observed (see Fig. 6a and b). This would suggest the presence of chemically mixed aerosols which grow at different rates as the humidity increases.

The possibility that the decrease in the height of the mixing layer reduces the dilution of the atmosphere has also been investigated. Temperature profiles from radiosonde taken at Beit Dagan about 15 km away from the sampling site indicated that at about 23:00 local time a temperature inversion occurred at the ground. The temperature increased with height to about 70 - 80 m and then decreased. Particles trapped in the lowest layer could not be mixed with air above, therefore increasing the aerosol concentration near the ground as shown in Figs. 6 and 7. Unfortunately, no temperature profiles had been taken at earlier times and one cannot be sure that the inversion at the ground was most responsible for the increase in aerosol concentration. This is further emphasized when the 5:00 A.M radiosonde data is analyzed. At that time no inversion was present and small convection cells were probably generated. This would suggest a decrease in the aerosol concentration near the ground. We see that this is so in Fig. 7a. On the other hand Fig. 7b shows a decrease in the aerosol concentration after 5:00 A.M and is therefore more closely correlated with the relative humidity. It is therefore difficult to conclude which of the two effects dominates. In Table 1 we listed some average values of C and β from Eq. 1 based on the summer measurements at Tel Aviv.

It should be pointed out again that the diurnal variations of the size distribution were also observed in the desert. However, only a very few such measurements are presently available, and these are not sufficient to allow us to draw firm conclusions.

d. Optical Properties and Composition.

Samples of atmospheric particulate matter were collected from the beginning of January 1976 to January 1980 (the sample collection is still continuing) by air filtration on 47 mm diameter 0.45 μ m pore size cellulose membrane filters, in order

to examine the composition and imaginary refractive index of the materials present. Details of the collection technique are available in a separate report (Petracca and Lindberg 1975). Casual examination of filter samples from the two collecting sites makes it immediately obvious that there is a considerable difference in the atmospheric particulate matter in Tel Aviv as compared to the site in the Negev desert. Samples from the desert are typically light brown or tan in color whereas those from Tel Aviv are dark grey or nearly black. Exception to this rule is observed during Sharav conditions (easterly wind) where the sample from Tel Aviv looks very much like the samples from the desert. A black and white picture of this is shown in Fig. 8. The Tel Aviv sample is similar in color to samples collected at other populated or industrialized areas in the world whereas the Negev sample is very much like examples collected in other rural semi arid regions.

We have examined the composition of these samples qualitatively by two methods. The first by infrared transmission spectroscopy, using the conventional KBr pellet technique with a Perkin-Elmer Model 521 dual beam spectrophotometer in the 2.5 to 30 micrometer spectral region. This method produces a transmission spectrum which can give a qualitative indication of the presence of significant quantities of substances present in the sample. Some materials known to be present in atmospheric dust such as sodium chloride or free carbon, do not have significant absorption bands in the infrared, and therefore cannot be detected by the KBr pellet method. From such spectra it is clear that samples from both sites contain significant amounts of gypsum, clay minerals, notably kaolin and montmorillonite clays, and in some cases, carbonate minerals such as calcite. There is no obvious general difference in the KBr pellet spectra between the two sites, although detailed variability does exist. Several examples are shown in Fig. 9. along with an indication of what minerals can account for the major absorption features. Note that the spectral detail, particularly in the 8-12 μm atmospheric region, is quite variable. This is because of variability of the relative amounts of particulate materials present in the sample. This can presumably be related to prevailing wind direction and origin of dust, but our data are currently not extensive enough to draw any conclusions of that nature.

In addition, several samples were examined for their elemental composition using a scanning electron microscope and an electron microprobe. The samples were

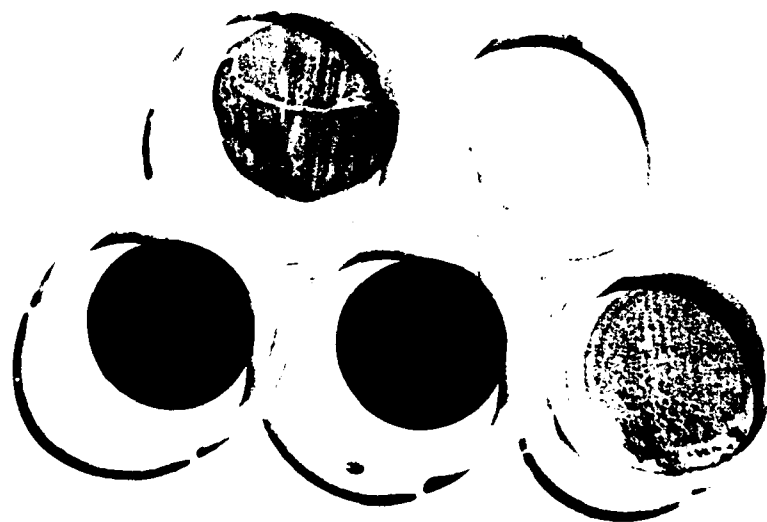
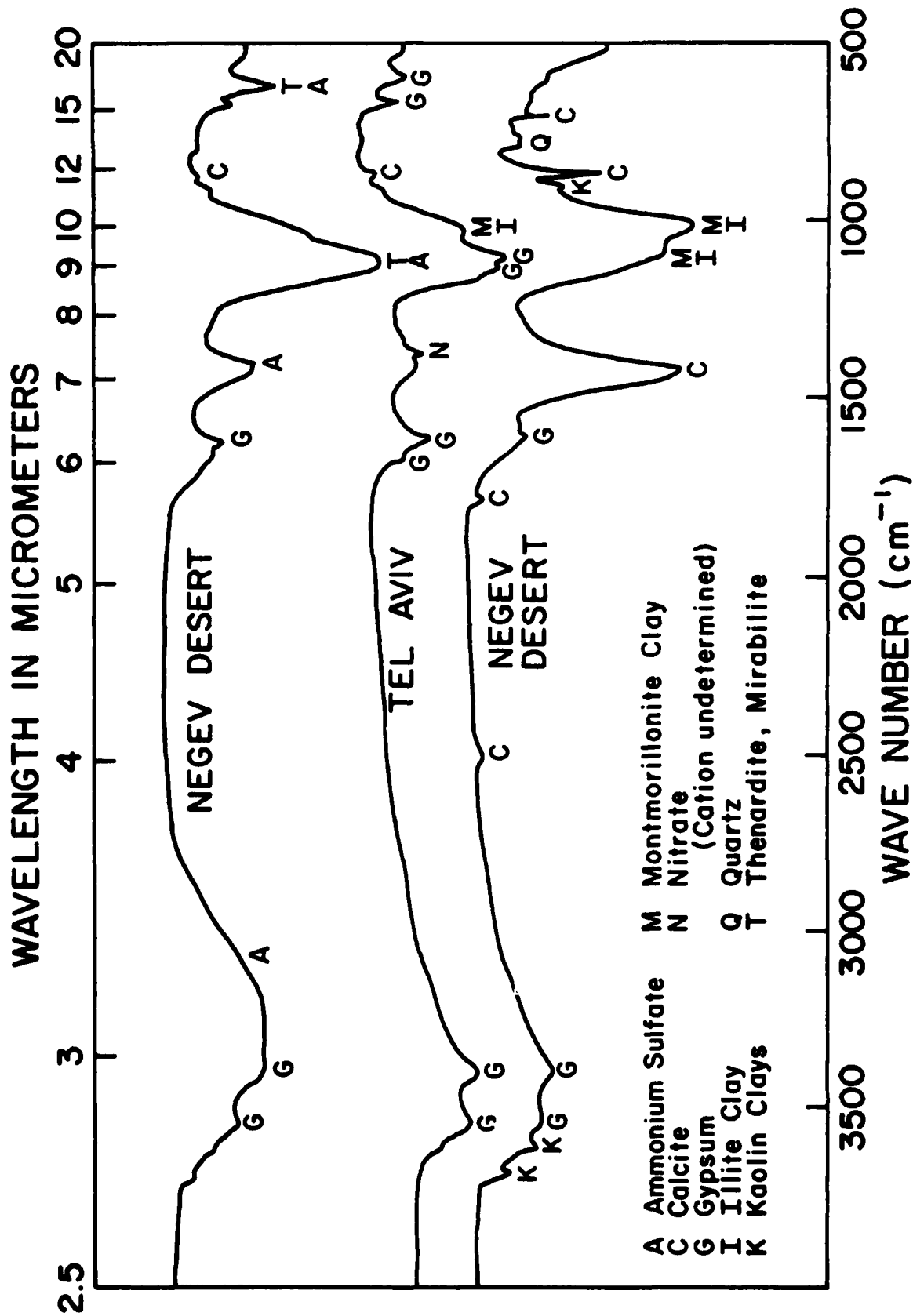


Fig. 8 Membrane filter samples of atmospheric dust from Israel. The upper two samples are from Mitzpe Ramon in the Negev desert. The bottom three are from Tel Aviv. The lighter of the three Tel Aviv samples (the one on the lower right hand side), shows the influence of persistent easterly wind conditions contributing additional desert dust to the normally dark appearing urban sample.

Fig. 9 Infrared potassium bromide disk transmission spectra of several atmospheric dust samples from Israel. These examples were chosen to show the kind of variability that occurs. The letters indicate the substances that can account for individual absorption features. Note the high degree of variability in the 8 to 14 μm spectral region.



coated with carbon so that no carbon could be detected in the analysis. These measurements indicate that during westerly flow the aerosols collected in Tel Aviv contain mostly Na, Cl, Si, Al and some S (Fig. 10a). On the other hand, during strong easterly flow and low visibility the aerosols primarily contain Al, Si, K, Ca and Fe (Fig. 10b). The elemental composition found in Tel Aviv during easterly flow is very similar to the one found in the Negev desert.

A semi-quantitative analysis of the relative abundance of the different elements with respect to Si was carried out using a wavelength dispersive microprobe. A comparison between aerosols from the Negev desert and Tel Aviv (under easterly flow) was conducted. Table 2 summarizes the X-ray count ratio of the different elements to Si using 100 seconds counting time (for some of the elements longer counting time was needed, but the total count was divided to comply with the 100 sec. standard).

From Table 2 we can see that no NaCl was found in the desert while an average of .4 Cl-containing particles per frame (100 μ m x 80 μ m) were observed on the Tel Aviv samples. It corresponds to about 1.5 particles per cm^3 of salt particles which are about $\frac{1}{40}$ - $\frac{1}{20}$ of the total aerosols loading within the size range that we measured. This is in contrast to a westerly flow condition in Tel Aviv where the NaCl concentration is high. Unfortunately, no samples taken during westerly flow conditions were available for the analysis with the wavelength dispersive microprobe. However, observations of such samples with the electron microprobe indicated the presence of relatively high concentration of NaCl-containing particles during westerly flow conditions, as expected.

From the analysis of the samples, we observed that certain elements were always present together. For example, Al and Mg were always present with silicates K with Si (but not with Ca), Fe with silicates and Ti with Fe. S was always found with Ca which suggests the presence of gypsum, in close agreement with our IR measurements (Fig. 9). The source of P in our samples is believed to be from the phosphate mining activities about 70 km to the NE of the sampling site.

In addition to the qualitative measurements discussed above, we have made quantitative measurements of the imaginary refractive index - which is equivalent to the optical absorption coefficient - for these particulate samples. This

Fig. 10a Electron micrographs of typical aerosol particles observed in Tel Aviv during westerly flow conditions (Sept. 1976). The elemental composition was obtained by an electron microprobe.



2 μm

Al, Si, Cl, K, Ca, Fe



NaCl

1 μm

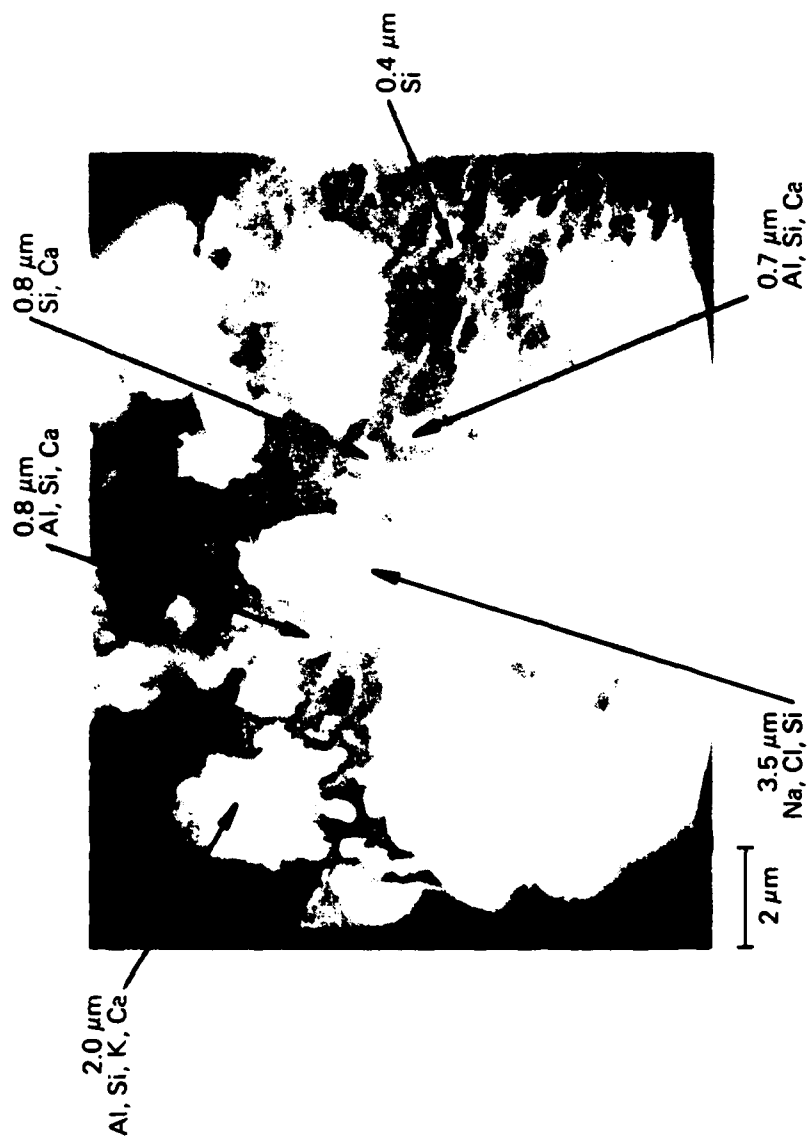


Fig 10b The same as Fig 10a except during easterly flow conditions on
Feb 4 1977.

Table 2. X-ray count ratio of different elements to Si

	Negev (Sept. 1976)			Tel Aviv (4 Feb 1977)		
	Photo 1	Photo 2	Photo 3	Photo 4	Photo 5	Photo 6
K/Si	0.46	0.50	0.65	0.19	0.37	0.29
Ca/Si	6.44	7.55	7.39	1.69	2.54	1.53
S/Si	0.20	0.17	0.28	0.08	0.11	0.09
P/Si	0.05	0.05	0.04	-	-	-
Ti/Si	0.04	-	0.04	0.02	-	-
Fe/Si	0.35	-	0.37	0.19	0.31	0.22
Cl/Si	-	-	-	0.06-0.09	0.07	0.06
Al/Si	0.35	0.45	0.41	0.24	0.28	0.28
Mg/Si	0.06	0.06	0.08	0.04	0.05	0.05
Na/Si	-	-	-	0.009-0.012*	0.016*	0.013

The symbol - indicates that the measurement was below the threshold of detection.

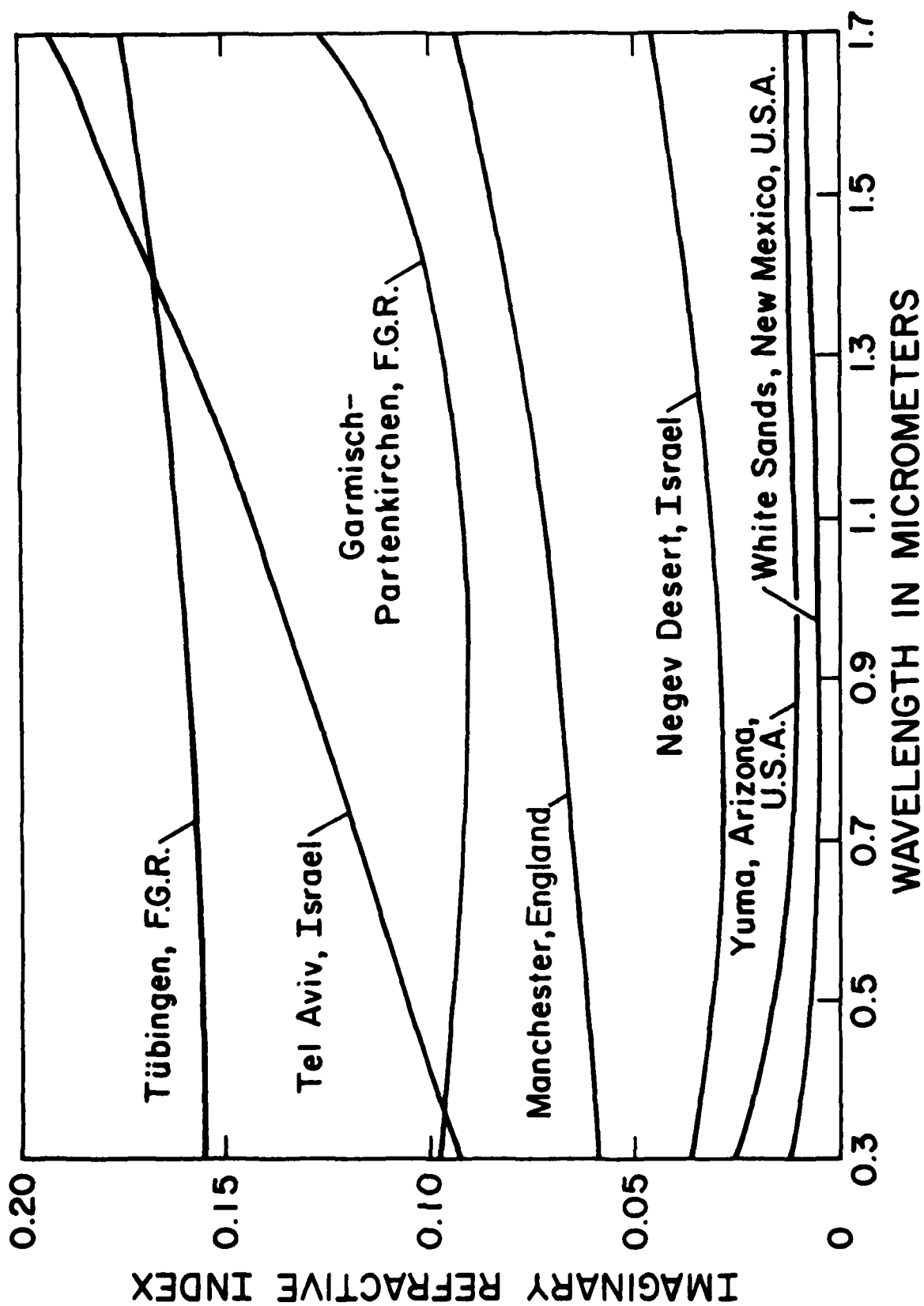
*Although counts of Na were not above background they appeared at exactly the location of the Cl. This suggested the presence of NaCl at low concentrations.

was done using a diffuse reflectance method developed earlier by Lindberg and Laude (1974) and by Lindberg (1975). In using this method it is first necessary to remove the dust sample from the membrane filter on which it was collected. This is done by dissolving the cellulose ester membrane in spectroscopic grade acetone. The acetone suspension is then centrifuged and most of the cellulose-acetone solution is removed by decantation. The particulate residue is then washed twice more with acetone to remove all traces of the cellulose membrane. It should be pointed out that particulate samples contain some organic substances that are soluble in acetone and are lost in this process. Therefore, the measurements reported here were made on the non-acetone soluble airborne particles.

After removal of the membrane the particulate matter is mixed with a highly refined form of barium sulfate powder so that the barium sulfate contains about one part in 10^3 atmospheric dust by volume. The barium sulfate initially is a nearly white powder with a known value of diffuse reflectance. The presence of the small quantity of atmospheric dust in the mixture reduces the diffuse reflectance of the powder, and a laboratory measurement is made of this degradation of reflectance. The instrument used was a Cary 14 spectrophotometer with an accessory integrating sphere for diffuse reflectance work, operating in the 0.3 to 1.7 μm spectral interval. From the reflectance data a value for the imaginary refractive index can be estimated, using equations based on the Kubelka-Munk theory of diffuse reflectance. Details of this computation are discussed thoroughly in the references mentioned above.

As one should expect from the appearance of the filter samples shown in Fig. 8, the imaginary index values we have measured are much higher for the Tel Aviv site than for samples from the Negev desert location. In Fig. 11 we have shown a typical example from each site in the 0.3 to 1.7 μm wavelength interval. For comparison we have also included several examples of similar measurements at other localities that were reported earlier by Lindberg et al. (1976). At any one site there is considerable variability, however, it can be seen that samples from rural semi-arid regions generally show lower imaginary indices than those from more urbanized, less arid areas. It seems reasonable to suggest that these differences are basically due to the relative proportions of natural and anthropogenic combustion or other pollution products and soil minerals present in the aerosol.

Fig. 11 Typical examples of the imaginary refractive index spectra for two atmospheric dust samples from Israel compared to several samples from other localities. In general samples from urban areas such as Tel Aviv and the three European sites shown show much higher imaginary indices than do those from the Negev desert or the two American desert localities (Lindberg et al., 1976).

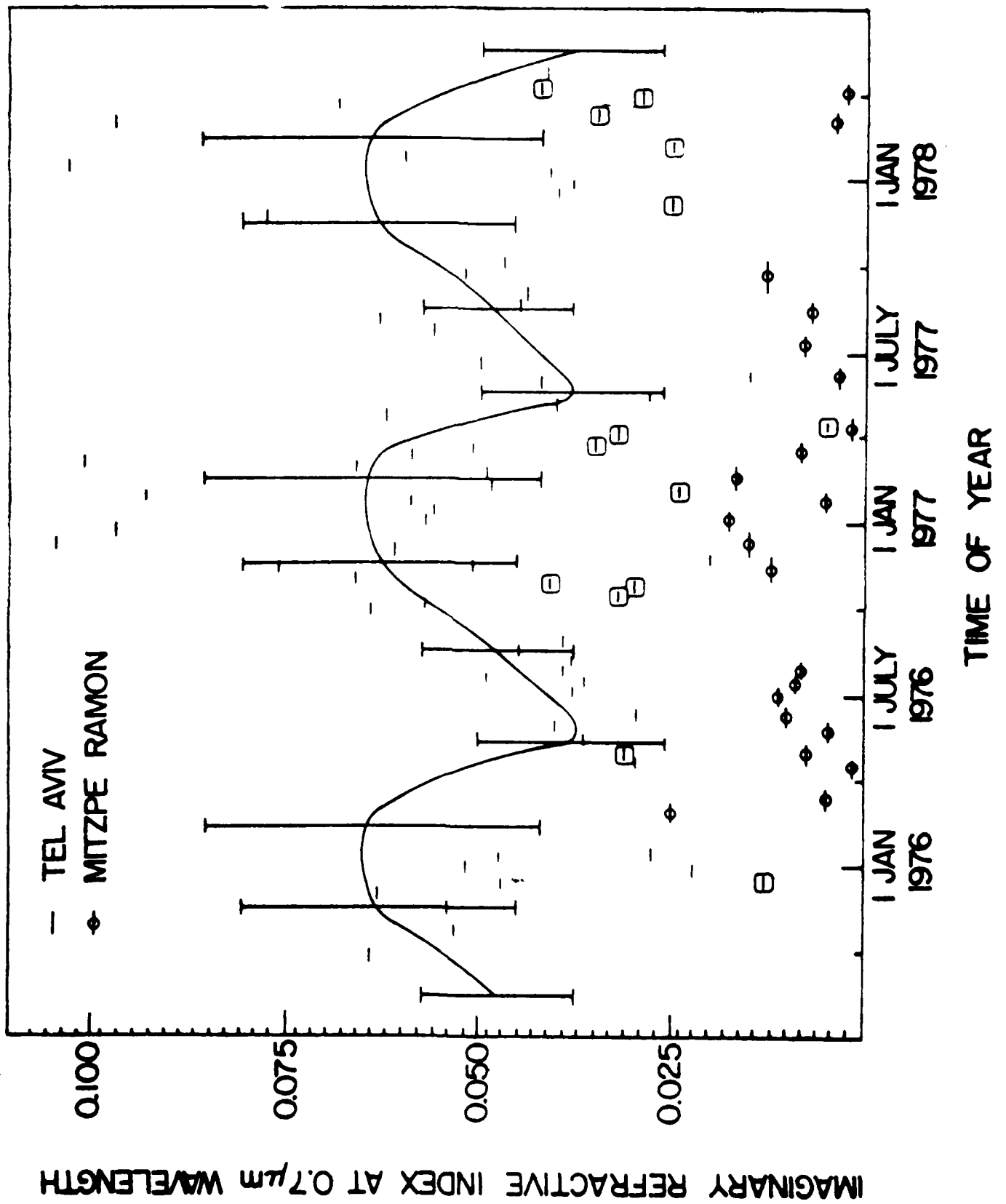


Patterson et al. (1977) have made measurements of the imaginary indices of Saharan aerosols using the same laboratory method. Their samples were collected from pollution-free island locations and on board the research vessel "Meteor" on both sides of the Atlantic Ocean. For a wavelength of $0.7 \mu\text{m}$, they obtained an imaginary refractive index value of about .004. As can be seen from Fig. 11 we have measured somewhat higher values for the Negev desert samples, the average of all 22 rural samples being about .008. We found considerable variability, with some as low as .002 and others as high as .024. This may imply that even in the Negev desert the aerosol is not completely free of more strongly absorbing materials and is still affected by the past history of the air mass involved. The Sahara aerosol measured by Patterson et al. being the result of severe dust storms in North Africa, is probably a rather pure mineral dust aerosol comparable to our Negev samples collected during high wind conditions. Examination of the meteorological conditions during the time our Negev samples were collected shows that during periods with high winds when the sample mass would have proportionately higher fraction of low imaginary index mineral matter, our imaginary index measurements are indeed the lower ones shown in Fig. 11, and have values comparable to the results obtained by Patterson, et al. This comparison again suggests that the actual imaginary index value is determined by the relative proportions of weakly absorbing mineral matter mixed with strongly absorbing substances such as natural and anthropogenically generated carbon and ash. Note for comparison that the aerosol samples from Tel Aviv in Fig. 11 show indices in the range from about .025 to .100.

We have also seen a seasonal variation in the imaginary index values, and this is shown in Fig. 12 which is a plot of measured values at $0.7 \mu\text{m}$ wavelength. In this figure each horizontal line shows an imaginary index value on the ordinant scale, and the length of the line indicates the time interval on the abscissa during which the sample was collected. Note that any time of year the values for the rural site in the Negev desert are always much lower than corresponding values for urban Tel Aviv samples. Also it can be seen in Fig. 12 that the imaginary indices are distinctly higher in the fall, winter and early spring months than during the summer months.

It is our view that when an air mass comes from a rural semi-arid region like the Negev desert the particulate matter is predominantly soil derived in nature, and has a low imaginary refractive index. For the Tel Aviv site however urban

Fig. 12 Imaginary refractive index values at $0.7 \mu\text{m}$ wavelength, for all of the atmospheric dust samples. The horizontal lines indicate the time interval on the abscissa during which the individual sample was collected. Note that in all cases those from Tel Aviv are much higher than values obtained nearly simultaneously from the Negev desert. There is also a clear increase in measured values during the winter months. The curve represents 3 months averages and the bars the standard deviation. The data points with squares were deleted from the averages since they represent samples which were strongly affected by dust from the desert during easterly flow in Tel Aviv.



pollution - particularly carbon particles of anthropogenic origin - add to the aerosol and greatly increase the resulting imaginary refractive index. This is the reason for the consistent difference in imaginary index between our two sampling sites. Based on observations made in other localities as shown in part in Fig. 11, one can state in general that rural arid regions show relatively lower imaginary indices than do industrialized urban localities.

There is considerable short term variability in the individual samples. This is because a short period of high wind or persisting easterly wind in Tel Aviv can add a significant amount of low index soil particles to the sample, and in effect dilute it so that the resulting measured value appears abnormally low. Examples of this can be seen in the cases of dust storms that occurred on April 23, 1976 and February 2, 1977. Both the Tel Aviv and Negev desert samples show unusually low values at these times and yet even in these cases the Negev samples have distinctly lower values. When the measurements taken at Tel Aviv during persisting easterly wind conditions and low relative humidities, have been deleted from the data (all data points in Fig. 12 with squares around them), and the remaining measurements averaged over a three months period, a clear difference is observed between winter and summer months.

The reason for this difference may be related to two factors. (1) During winter months a low morning inversion occurs (lower than in the summer). This would prevent pollutants from escaping or diluting with the air above. Sampling during these periods increases the amount of aerosols collected. Since most of these particles originate from anthropogenic sources, their refractive index is usually higher, causing the higher values obtained during winter months. (2) It is also possible that some aerosols generated in Europe are transported to the Eastern Mediterranean with the general circulation patterns common during winter months (e.g. Gagin, 1971). Since the European air mass has a much higher proportion of pollution products as compared to soil matter than does an air mass originating further south, one would expect a higher imaginary index in Israel during the winter months. In the summertime the Eastern Mediterranean is in a region of subsidence and most of the particles that are found originate from either the sea or from the arid regions of North Africa. Thus one should expect lower imaginary index values for the summer measurements. This is consistent with our observations to date.

However, there are other factors which can have a bearing on the observed seasonal variation, such as differences in average wind speed - and thus the contribution of soil particle to the aerosol - or seasonal variations in the activity of anthropogenic particulate sources in Tel Aviv. There is some indication of this in our data. In December 1976, the imaginary indices for Tel Aviv were much higher than earlier, and this occurred at a time of year when residential heating begins, thus contributing free carbon particles to the urban aerosol. However, since home heating only starts in late November or early December, while our measurements indicate a rise in the imaginary indices in September-October, we feel that changes in local output of pollution could only be secondary in magnitude to the general circulation and local meteorological effects.

e. Summary of Observations.

Measurements of aerosols and their properties were carried out at two cities in Israel. The two sites were selected to represent urban and desert regions. The city of Tel Aviv was chosen as an urban region and Mitzpe Ramon (Negev desert) as representing a desert region.

Three types of measurements were carried out: (1) Size distribution of aerosol particles, (2) their chemical composition, and (3) their optical properties.

Data of the size spectra in both locations were fitted with a Junge-type distribution for presentation of their time variations. The winter aerosol concentrations in Tel Aviv were found to be about one order of magnitude higher than those from Mitzpe Ramon. The data indicates also that the exponent, β , is higher in Tel Aviv than in the desert. This is somewhat expected since particles in urban environment usually contain higher concentration of small particles originating from gas to particle conversion.

In addition to the differences between Tel Aviv and the desert we observed diurnal variation of the aerosol size spectra between day and night during the summer in Tel Aviv. These variations are believed to be related to either the growth of the particles by water absorption during high humidity events or due to a decrease in the height of the mixing layer during the night.

Measurements of the chemical composition were carried out by infrared absorption spectroscopic measurements of the samples which had been collected on filters. In addition, samples which had been collected on other filters were used for analysis by electron microprobe and by wavelength dispersive probe. The last two methods show some variation between samples collected in the desert and those collected at the Tel Aviv site. Samples from the desert show the presence of calcite, clay minerals and gypsum and the lack of NaCl. This is typical of desert aerosols. The Tel Aviv samples show strong variation with the synoptic conditions. During Sharav conditions (Khamsin) in which the winds in Tel Aviv are primarily from the east, the aerosols found in Tel Aviv are very similar to those found in the desert samples. However, during normal meteorological conditions which are dominated by westerly flow, the aerosols samples were found to contain large amounts of NaCl particles from the sea, together with soil-type aerosols originating from the North African deserts.

We have also shown that both seasonal changes in aerosol composition and differences due to geographic location (proximity to anthropogenic pollution sources) in Israel can result in measurable changes in the visible and near infrared spectral region imaginary refractive indices of atmospheric particulate samples. Those samples collected in Tel Aviv always exhibited imaginary indices two to four times as large as did samples collected at similar times in the Negev desert. In Tel Aviv, there is a distinct increase in imaginary index values during the winter months. To a lesser extent this seasonal change can also be seen in the measured values from the desert site as well. These variations appear to be related to vertical temperature structure of the atmosphere during those seasons, and probably also to the geographical areas over which the air masses coming to Israel have passed.

f. Conclusions

All of these observations are consistent with the following view of the aerosol prevailing in this area. Suppose that a background of desert aerosol with its relatively low imaginary refractive index and typical size distribution is present at both locations. Then we further suggest that the urban site at Tel Aviv has added to it particles of anthropogenic origin, typically carbon

particles from combustion residue. These particles, being much smaller in size than soil-derived desert aerosol particles, not only account for the observed higher number density in Tel Aviv, but the larger slope of the size distributions (evidenced by higher β values) as well. The pollution particles also explain the significantly greater imaginary refractive index of the Tel Aviv samples, since carbon particles have imaginary indices that are orders of magnitude higher than typical soil minerals. This view is further supported by the observation that both sites exhibit relatively higher imaginary indices during the winter months when low temperature inversions occur and when Israel is in the path of presumably more polluted air from southern Europe than they do during the summer months when the mixing depth is greater and also when Israel is in the flow of desert air from North Africa or the Sinai deserts. The variations in optical properties and size distributions of aerosols in Tel Aviv with prevailing local meteorological conditions are also explainable on this basis. For example, when wind conditions are high and from the desert area the strongly absorbing urban aerosol in Tel Aviv is diluted to some extent by weakly absorbing desert soil particles of larger size. Thus the overall imaginary index is lowered in Tel Aviv, and the size distribution shifts to larger particles.

It appears from our observations that the physical, chemical and optical properties of the atmospheric aerosol in Israel can be described as a combination of natural desert aerosol modified in some areas by urban anthropogenic contributions and by synoptic scale movements of air masses from Europe or the Mediterranean Sea.

Part II: Properties of Sharav (Khamsin) Dust-Comparison of Optical and Direct Sampling Data.

a. Introduction:

Windblown dust is one of the major sources or components of natural and man-made aerosols in the atmosphere (e.g. S.M.I.C. 1971, Carlson and Prospero, 1972, Carlson 1976). Desert dust is in turn an important part of dust aerosol and of the so-called "background aerosol"; its source regions cover one third of the world's land surfaces (Flohn 1970) and its sinks are global (Goldberg, 1971 Shipley et al 1975).

There is much intrinsic interest in the investigation of the physical and chemical properties of the desert aerosol with a view to evaluating the latter's potential direct and indirect climatic effects in our and other planetary atmospheres, (e.g. Joseph et al, 1973, Joseph and Wolfson, 1975, Joseph 1976, Joseph, 1977, Carlson and Prospero, 1972, Kondratyev et al, 1973 and De Luisi et al, 1975a,b).

Most experimental studies of the desert aerosol, or of any aerosol, suffer from the fact that it is fairly difficult to study a 'pure' mono-source natural aerosol without admixtures of other aerosols, clouds or gases.

This part of the report concentrates on a case study in which it was possible to isolate clearly one single aerosol type. We carried out simultaneous in-situ measurements of aerosol size distributions, imaginary part of the refractive index as well as of spectral transmission of the atmosphere to solar radiation.

The simultaneous time-histories of some of these quantities will be presented and inter-compared. Furthermore, the results will be compared with relevant data in the literature.

A severe Sharav (Khamsin) dust storm occurred on June 6, 1977 brought on by the passage of a thermal low pressure system coming from the North Africa deserts, over Israel (see Fig. 13a and b). The cold front seen in the figure passed the observing site at about 12.00 noon. Winds were mostly from the S - SW before the frontal passage and did not exceed 5 m sec^{-1} at our station. After the front passed, the wind shifted to more westerly flow with speeds of up to 10 m sec^{-1} . No clouds were observed during the major part of the storm and the relative humidity decreased

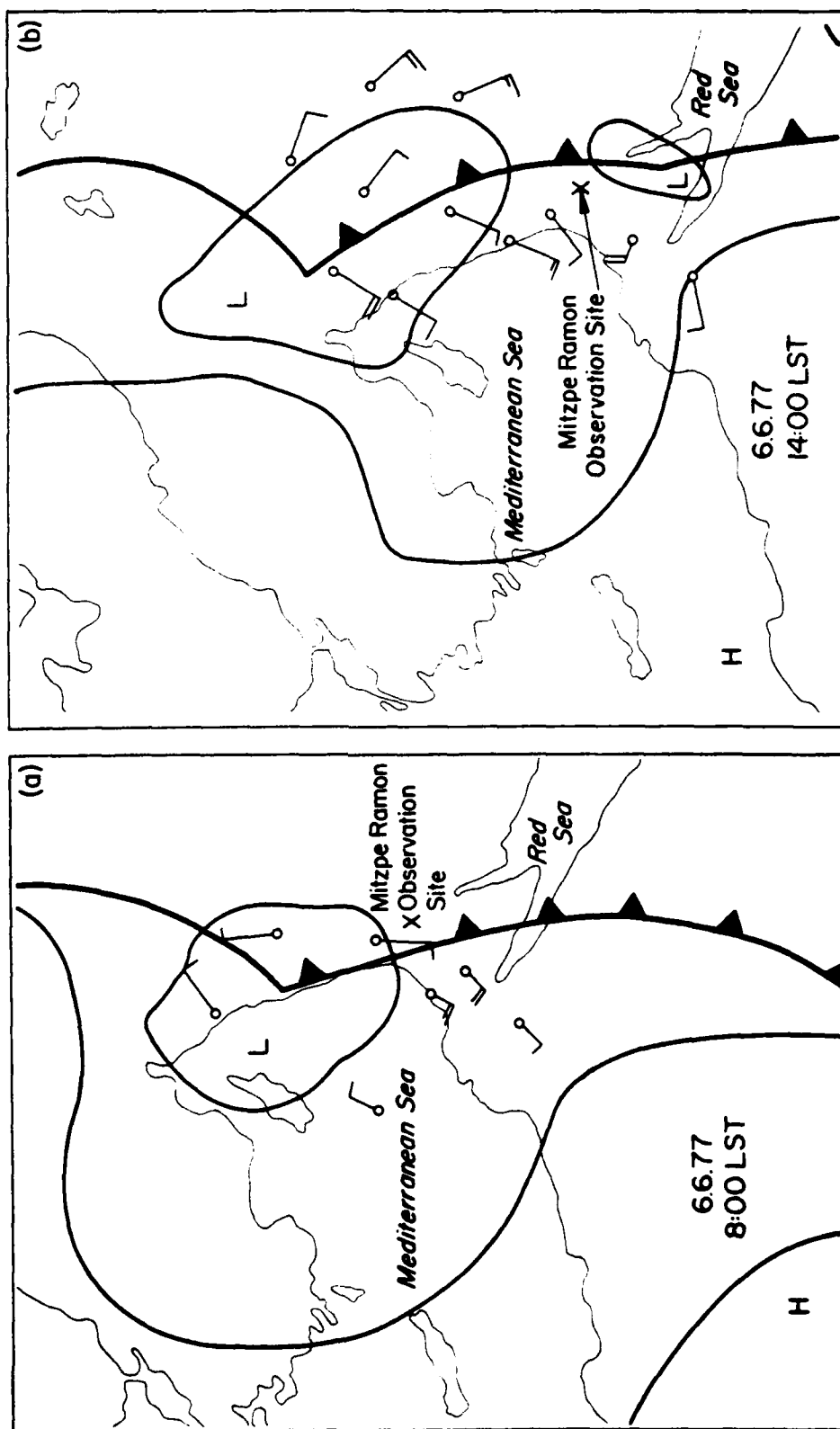


Fig. 13 Synoptic maps of the Weather Situation on 6/6/77, (a) 8:00 LST and (b) 14:00 LST

continuously from the morning (51% at 8 LST) to evening hours (17% at 20 LST). The observed optical depths were larger than one and reached values larger than three, thus making the aerosol by far the dominant absorber and scatterer of solar radiation.

The dust first appeared at higher altitudes before it was detected at the surface. This resulted in a low vertical visibility (milky white sky) and horizontal visibility of 40-50 km from the morning hours until about 11.00 LST when the horizontal visibility decreased and varied between values of 1 to 10 km.

b. The Data Acquisition Systems

The experimental systems were set up at the Astronomical Observatory of Tel Aviv University near Mitzpe Ramon in the High Negev Desert (Lat. 30.596N Longitude 34.762E at about 900 meters above M.S L.). Aerosol size distributions were measured automatically every 15 minutes (as was described in the first part of this report) during the day and night with the Royco optical counter (Model 220) placed on the roof top of the observatory (5 meters above ground). The instrument had been well calibrated, prior to the field experiment, with dry latex particles (Levin and Lindberg, 1979, and Part I of this report).

The aerosols were also collected on millipore filters (0.45 μm pore size) for later analysis of the imaginary part of the refractive index as a function of wavelength in the visible. Due to the need for relatively large amounts of dust for this analysis, the sample was collected over a 14 day period which included the Sharav day. The optical analysis of the samples was carried out by the Kubelka-Munk reflection spectroscopy technique (Lindberg, 1975) at the U.S. Army laboratories at White Sands.

Solar radiation measurements were taken with a six channel sun-following automatic spectro-radiometer equipped with six interference filters of 0.01 μm half width (see Figure 14). The solar radiation is collimated to provide an effective field of view of 1° .

The collimated solar radiation is chopped and detected by a sensitive silicon photo-diode with a broad spectral response curve (UDT 450) and recorded digitally on paper tape. Each set of spectral data is obtained in two minutes.

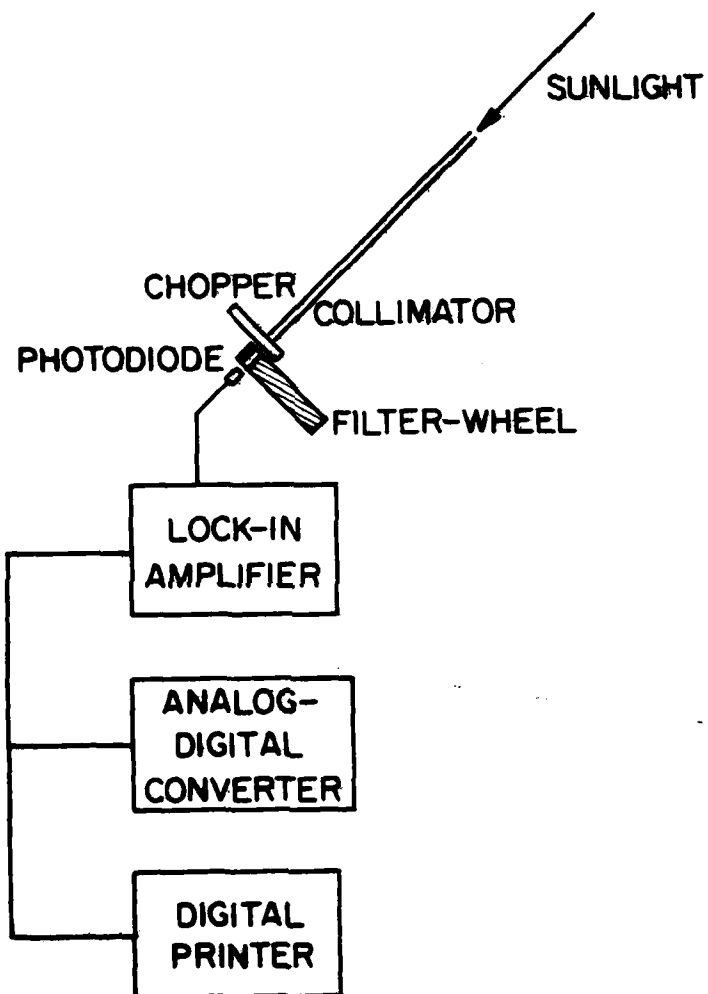


Fig. 14 The Normal-Incidence Sun-Following Automatic Interference Filter Spectrophotometer.

Observations of transmitted solar intensity, $I(\lambda)$, in all wavelengths were taken every half-hour to hour, depending on the rate of change of the solar zenith angle, θ_0 , with time, starting with solar zenith angles of about 75 degrees.

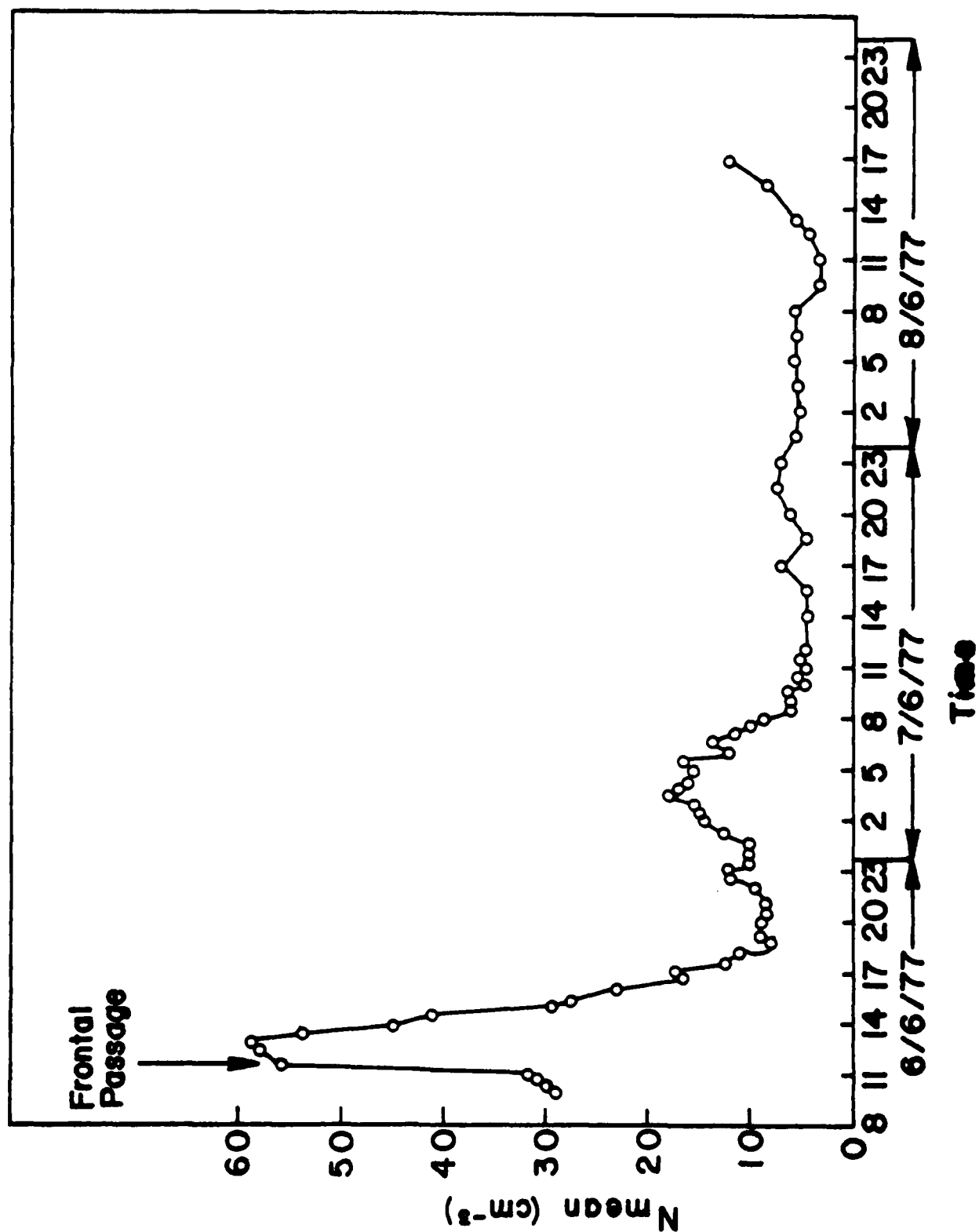
The instrument is regularly calibrated with a secondary standard (ISCO Model SRC 1601S), aged and run under standard conditions as specified by the manufacturer. A second, independent method of calibration is by use of a Langley plot extrapolation to $\sec\theta_0 = 0$ of a set of measured intensities, I , at a given λ , on a $(\log I \sec\theta_0)$ plot on optically stable clear days. These data, I_0 , are determined by a least-square technique at each wavelength and used as a calibration whenever their average relative RMS error is less than 3%. (e.g. King et al, 1978).

Measurements of surface temperature and humidity as well as pressure and wind were available. Radiosonde data were also available from Beit-Dagan (about 170 km away).

c. Data and Analysis

1. Size Distribution.

Measurements on the surface of the aerosol size distributions suggest that large changes occur in the latter during the passage of the front. The curves with open circles in Fig. 15 and in Fig. 20a present the mean total number concentrations (mean of 4 measurements every 15 min.) as a function of time as determined by the Royco counter. We clearly see the sharp increase in aerosol concentration during the passage of the cold front (see Fig. 15). The atmospheric aerosol load began to increase even before 10:00 A.M. (about $1\frac{1}{2}$ hours ahead of the front), and decreased sharply over a few hours following the frontal passage. The change of aerosol concentration with time is similarly shown in Fig. 16 which presents detailed size distributions. One can see that the peak of the size distribution around $1 \mu\text{m}$, becomes very prominent around the time of the passage of the front, and disappears gradually afterwards. The average slope of the distribution between $2 - 10 \mu\text{m}$ remains approximately constant for over a day at a value of about 2.3. Only two days later does the slope approach that of a typical distribution for the region, (marked average winter day on Fig. 16. A closer look reveals that at 10:00 A.M on June 6 (prior to the passage of the cold front) a flat-top



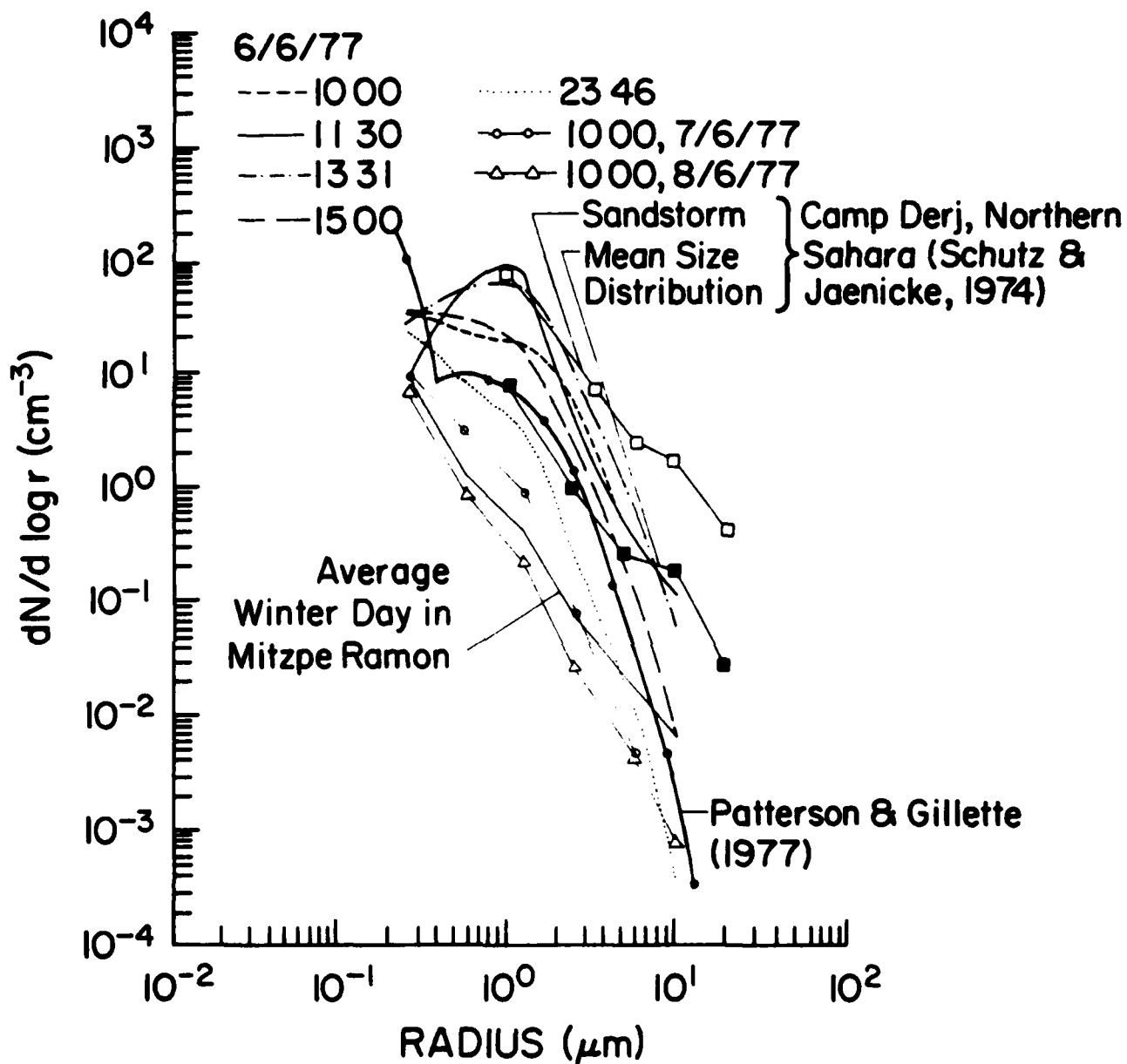


Fig. 16 Size distribution, $\frac{dN}{d \log r}$, of desert aerosol measured at surface level at Mitzpe Ramon, 6-7-8 June 1977 with a Royco 220.

distribution (over the range $0.15 - 1.5 \mu\text{m}$) had developed as a result of the increase in the number concentration of particles around $1 - 1.5 \mu\text{m}$ in radius. This increase is further emphasized at 11:30, just prior to the passage of the front when a maximum around $1 - 1.5 \mu\text{m}$ had developed. One should also note the slight increase in the number concentration of the largest particles ($\sim 10 \mu\text{m}$) which suggests the presence of a second peak at larger sizes, not resolved by our instrument.

Comparison of our data, after the peak of the Sharav, (e.g. 15:00 LST onward), with the aerosol size distribution measurements at Haswell, Colorado as reported by Patterson and Gillette (1977) (P.G. from here on) shows the similarity of the distributions at the two locations within the range of our measurements. On the other hand, the differences in the concentrations of aerosols of sizes around $1 \mu\text{m}$ during the storm in comparison to both the post Sharav conditions and to P.G.'s data are obvious: our distributions have large variations in the peak at $1 \mu\text{m}$. For comparison we plotted the size distribution which was measured during dust storm conditions at Camp Derj Northern Sahara by Schutz and Jaenicke (1974) as well as their mean size distributions. These distributions have smaller slopes than the ones we observed during the peak and after the passage of the dust storm. In fact their slopes more closely resemble the slope of average size spectra taken during a winter day in the Negev desert. On the other hand, the number concentrations of the $1 \mu\text{m}$ particles measured during the dust storm in the Sahara agree with our measurements during the period of maximum aerosol loading. The differences between the distributions probably stem from the differences in the wind speeds and hence in the intensities of the dust storms and in the composition and structure of the soils. When the data is plotted as volume distributions, we observe in Fig. 17 the appearance of a double mode. We have plotted here the volume distributions for some of the curves presented in Fig. 16. In addition P.G.'s "Typical" volume distributions of heavy and light desert aerosol loading are presented. Our post-Sharav distributions fall within their two, somewhat extreme values. The shapes of most of our curves, except those at 10:00 and 11:30, around the passage of the cold front, agree with the general shape of P.G distributions between $0.3 - 10 \mu\text{m}$. The measurements at 10:00 and 11:30 LST (during conditions of heavier aerosol loading) have a double mode distribution; both modes located at somewhat smaller radii than those of P.G. for heavy atmospheric loading. The

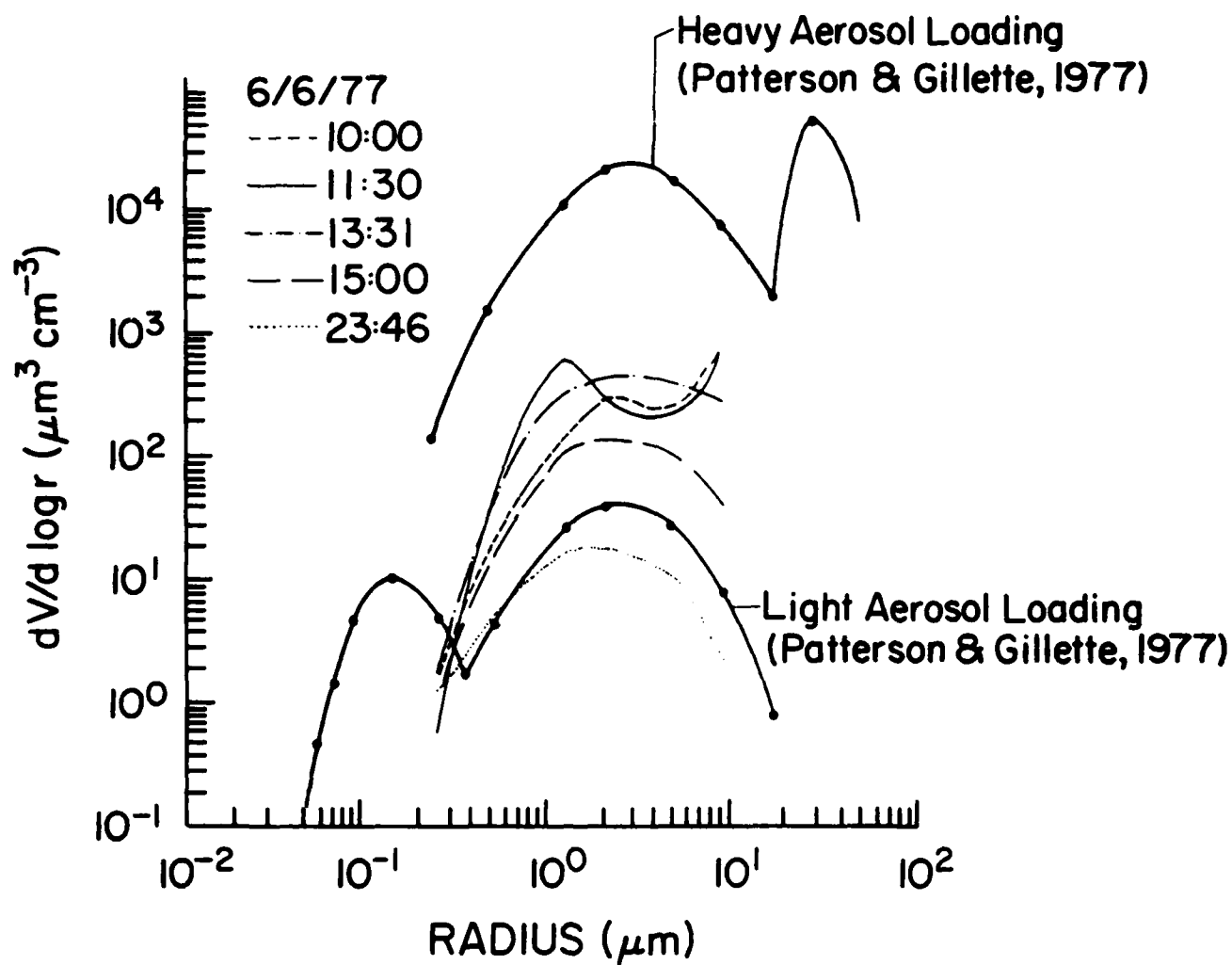


Fig. 17 Volume distributions, $\frac{dV}{d \log r}$ under conditions of Fig. 16.

increases in particles in the range between 1 - 10 μm is thought to be characteristic of the occurrence of soil derived aerosols under all conditions. The appearance of the second peak at larger radii under higher wind speed conditions, is believed to be a result of locally generated dust, and may be related to the characteristic size spectra of the parent soil. It is correlated with the strong decrease of horizontal visibility observed during that period (see next section).

Figure 18 presents the area distributions at various times in comparison to the area distributions obtained by P.G for moderate aerosol loading in Plains Texas. If one uses the P.G definitions, one sees that our Sharav can be classified as an event of moderate aerosol loading. However, one should clearly note that the peaks of all our area distributions during the passage of the storm are lower than that of P.G. Also the appearance of the second mode around 11:30 LST shows up at considerably smaller sizes than those shown by them.

The general conclusions that can be drawn from these measurements are (1) The Sharav produced moderate aerosol loading when compared to the scale suggested by P.G, although the optical depth was very large in our case. (2) Just prior to and during the passage of the front, a sharp increase in the aerosol content is observed. (3) The shape of the size distribution is similar to that reported by other investigators, mainly for measurements taken a few hours after the front had passed (4) Just prior to and during the passage of the front, the size distribution developed a double mode. This development is a result of locally blown dust and causes the peak of the size spectra to shift to larger radii (Chepil and Woodruff, 1963). (5) The general shapes of the volume and area distributions also show that the aerosol loading produced by the Sharav was moderate in intensity on the P.G scale. (6) The commonality of the size distributions found by P.G for soil derived aerosols are upheld by our measurements primarily for post Sharav conditions. However, different distributions from those of P.G appear at times around the passage of a cold front.

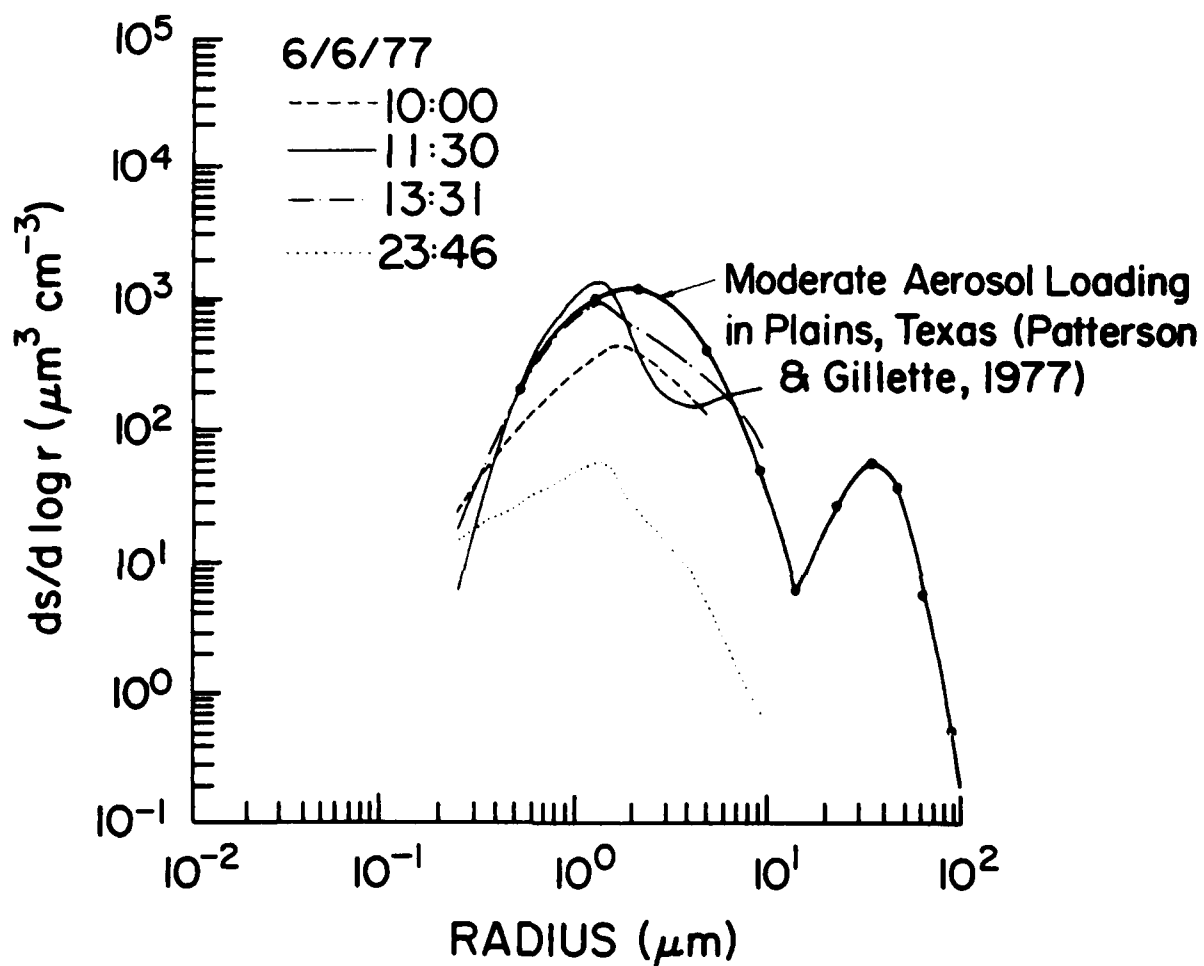


Fig. 13 Area distributions $\frac{ds}{d \log r}$, under conditions of Fig. 16.

ii. Imaginary Refractive Index

Figure 19 represents the imaginary refractive index in the visible as measured by the reflection technique (Lindberg, 1975). As can be seen the values of this parameter during Sharav are considerably lower than those observed at the same site under clear conditions (Levin and Lindberg, 1979, and the first part of this report). However, they are fairly similar to those observed at White Sands. This suggests that the higher values observed in the Negev desert under clear conditions stem from the fact that the aerosols are composed of desert type particles together with a small fraction of highly absorbing urban aerosols. Under clear conditions our Negev site is affected by winds from the North and Northwest during the course of each day. The air coming from these directions carries pollutants from coastal and inland cities. On the other hand, during the Sharav itself, desert aerosols dominate. These, being particles of low absorption, cause a drastic reduction in the imaginary refractive index. The similarity between the absorptivities in the visible range during Sharav conditions and those measured at White Sands suggest that pure desert aerosols have very low absorption (in the visible) regardless of their sources. This commonality in the imaginary refractive index is very important for evaluation of global or regional effects of desert aerosols.

It should be pointed out that a fair amount of commonality is also observed in the thermal I.R. absorption spectra. All desert aerosols show strong absorption peaks in the 8 - 12 μm atmospheric transparency window (e.g. Volz, 1973, Shipley et al, 1975, Fischer, 1976, Levin and Lindberg, 1979). The variations in the wavelengths of the absorption peaks stem from the temporal and spatial variations in the chemical composition of the particles at the various sites of observation.

iii. Spectral Transmission of the Atmosphere.

The optical measurements undergo the following analysis. Each measurement set, automatically acquired in two minutes, is composed of two spectral scans - 0.4 to 1 μm and 1 to 0.4 μm , two determinations of the dark current and of the time - one at the beginning and one at the end of the set.

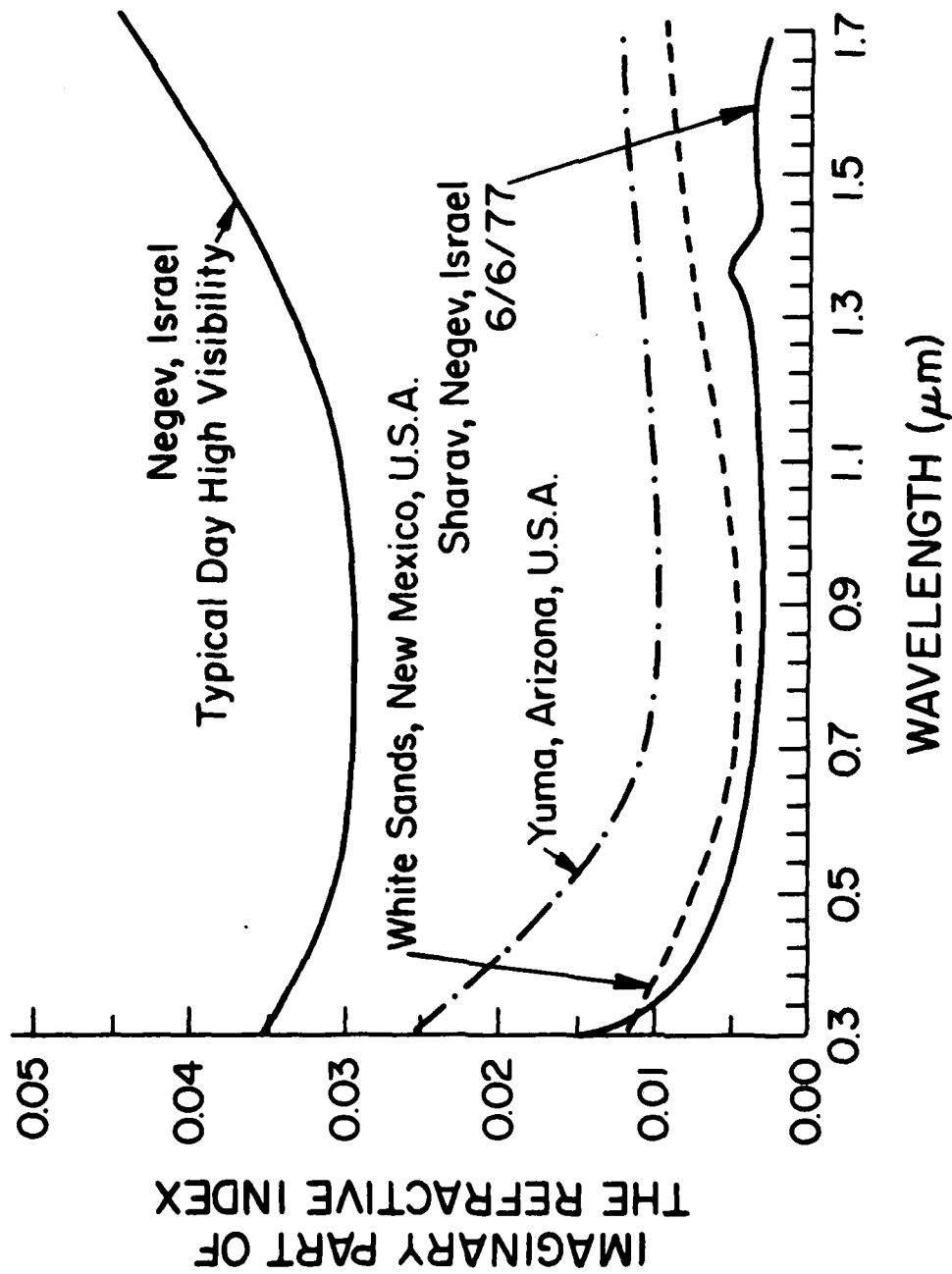


Fig. 19 The imaginary part of the refractive index in the solar spectral range during the period of the storm.

One then calculates the average of each two spectral measurements, of the dark currents and of the time.

The aerosol optical depth, $\tau_D(\lambda)$, at each wavelength, is then calculated from the averaged measurements by use of the following equation

$$\tau_D(\lambda) = \left(\ln \frac{I(\lambda)}{I_0(\lambda)} - \tau_R(\lambda) \frac{P}{P_0} - \tau_{O_3}(\lambda) \right) \sec \theta_0$$

where

$I(\lambda)$ = measurement of solar direct flux at wavelength λ ;

$I_0(\lambda)$ = measurement at top of atmosphere; (from each day's calibrations, that of the previous day or from an absolute calibration;

$\tau_R(\lambda)$ = Rayleigh optical depth at wavelength λ ;

P/P_0 = Pressure in units of standard pressure;

$\tau_{O_3}(\lambda)$ = Ozone optical depth: climatological averages are used.

We assume that atmospheric forward scattering effects in the field of view are negligible (e.g. Grassl, 1970) and that we may use $\sec \theta_0$ for the effective air mass at all measurement times (valid for $\mu_0 > 0.25$) and for all scatterers and absorbers (strictly valid if all well-mixed). The actual value of the air mass, $\sec \theta_0$, is calculated from the average time of the measurement and the location of the station.

The values of $\tau(\lambda)$ for $\lambda = 0.45, 0.55, 0.65, 0.85$ and $1.0 \mu m$ are prepared in two ways for further analysis. First, we calculate

$$R(\lambda) = \frac{\tau(\lambda)}{\tau(0.45)} \text{ to make the data independent of total amount.}$$

$R(\lambda)$ is then fitted logarithmically to

$$R(\lambda) \cong A \left(\frac{\lambda}{0.45} \right)^{-\alpha}$$

by the method of least squares. This is done to facilitate comparison to the large volume of data available in the literature, derived both empirically and theoretically, in the form

$$\tau = \beta_0 \lambda^{-\alpha}$$

where $\alpha \geq 0$ in many cases (Angstrom, 1929, 1961. Junge, 1963, Deirmendjian 1969 etc.) but may also be negative.

We added the factor A to indicate the possible departure ($A \neq 1$) of the optical depth from that for a simple power-law size distribution. Such departures occur especially in the size range $0.1 \leq r < 2 \mu\text{m}$ to which the optical measurements are most sensitive, (e.g. Junge, 1972, Schutz and Jaenicke, 1974, Twitty et al. 1976. DeLuisi et al. 1975a,b).

Some of the data is summarized in Fig. 20 and in Table 3. Part (a) of Fig. 21 shows the variation of two optical depths, at two wavelengths, $\tau(0.45)$ and $\tau(0.65)$, with time on the day of the Sharav (Khamsin), June 6, 1977, and for two days afterwards. All optical depths increased to values larger than 3 during the dust storm, almost independently of wavelength. The relative independence of the optical depth of wavelength is also shown in Fig. 21b and Table 3 -- is close to zero during the storm. After the storm, the optical depths were only weakly dependent on wavelength on June 7 and again almost neutral on June 8, when a weak dust storm developed (see also Table 3 and Fig. 20).

The optical depth during the two days following the storm was almost an order of magnitude smaller, although still higher than normal for the time of year. (Joseph and Manes, 1971, Joseph et al, 1973).

The parameter A was significantly different from one. (see Fig. 20c and Table 3), showing that the size distribution was different from a simple power law. The power, α , (Fig. 21 and Table 3) of the average wavelength dependence was close to zero and negative on June 6, showing that the particles were fairly large. These results are corroborated by the Royco measurements. On the two days following the storm, α climbed to 0.2 - 0.5. which is still much lower than normal. (Joseph et al, 1973).

Fig. 20 The total mean number density, N (as in Fig.15), the optical depth at wavelength $0.45 \mu\text{m}$, τ_1 (a); the constant C of the average power-law size distribution (Eq. 1), (b); the constant A of the average wavelength dependence of the optical depth $(\tau(\lambda) = \tau_1 A (\frac{\lambda}{0.45})^{-\alpha})$ (c); the average slope of the size distribution, α , derived from in situ (Royco) and optical data (d).

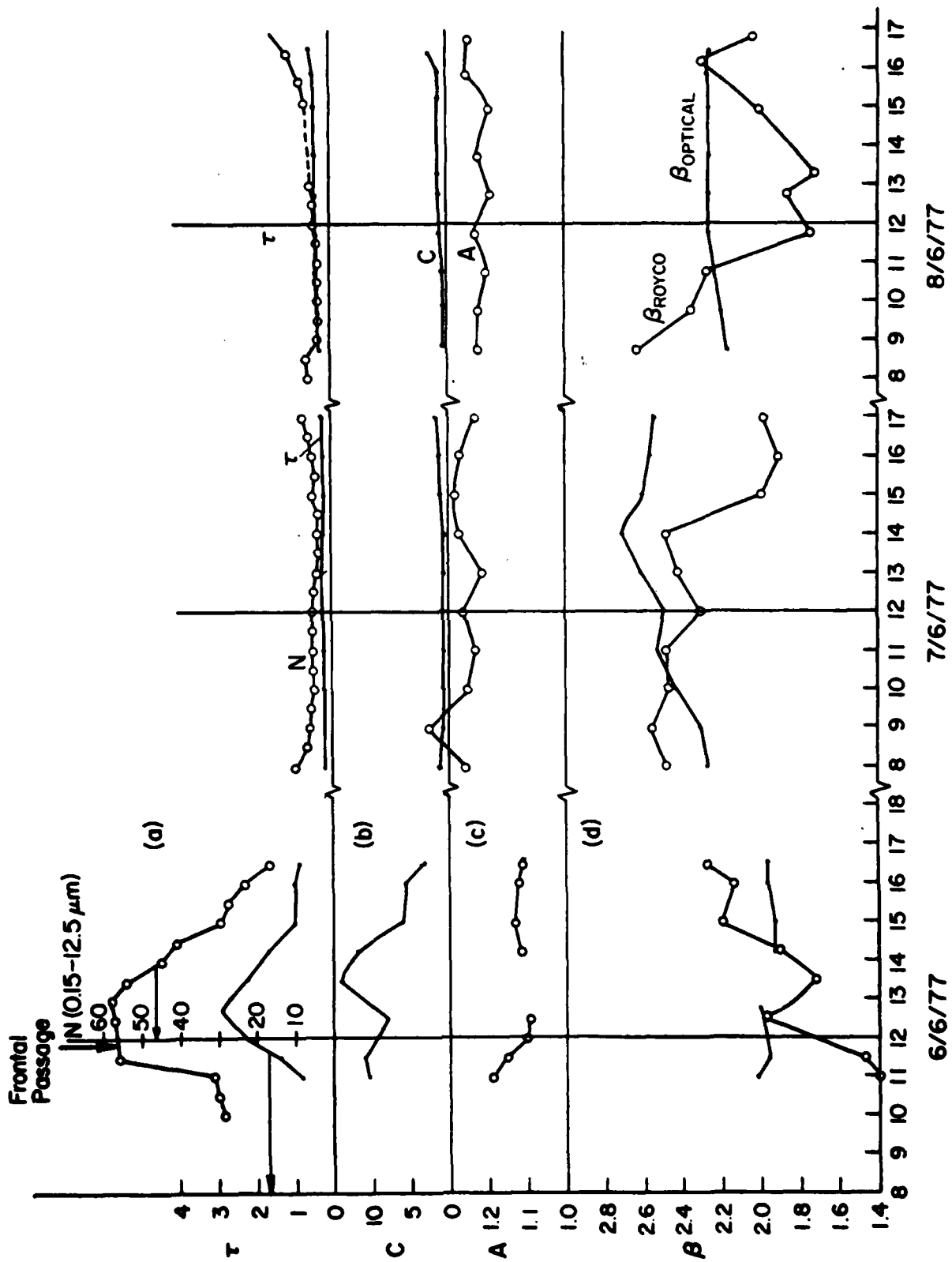


Table 3 - Properties of Aerosols on June 6-8, 1977

(a) - Fit to power-law size distribution $\frac{dN}{d\log r} = Cr^{-\beta}$

Date	Time	μ_o^{-1}	$\tau(0.45)$	$\$A$	$\$a$	β_{optical}	β_{Royco}	β_{Royco}
6/6/77	1100	1.037	0.84	1.19	0.45	2.05	1.38	10.60
	1130	1.016	1.33	1.15	-0.04	1.96	1.46	10.13
	1200	1.009	2.30	1.10	-0.04	1.96	--	--
	1230	--	--	--	--	--	1.97	7.93
	1245	1.025	2.87	1.09	0.003	2.00	1.84	--
	1330	1.075	2.22	--	--	--	1.71	13.80
	1415	1.168	1.69	1.11	-0.08	2.92	1.89	11.77
	1505	1.342	1.02	1.13	-0.08	1.92	2.19	5.91
	1550	1.606	1.00	1.12	-0.04	1.96	2.13	5.54
	1630	2.00	0.90	1.11	-0.05	1.96	2.27	3.12
7/6/77	0805	1.636	0.21	1.26	0.27	2.27	2.48	0.85
	0900	1.316	0.21	1.35	0.30	2.30	2.55	0.53
	1000	1.129	0.23	1.25	0.43	2.43	2.46	0.53
	1100	1.037	0.20	1.23	0.52	2.52	2.48	0.52
	1200	1.009	0.24	1.26	0.49	2.49	2.30	0.56
	1255	1.033	0.25	1.21	0.61	2.61	2.42	0.37
	1405	1.142	0.22	1.27	0.70	2.70	2.48	0.37
	1500	1.319	0.22	1.28	0.60	2.60	1.99	0.77
	1600	1.683	0.22	1.27	0.56	2.56	1.90	0.85
	1700	2.479	0.25	1.23	0.54	2.54	1.98	1.56
8/6/77	0845	1.385	0.29	1.22	0.17	2.17	2.63	0.35
	0945	1.165	0.33	1.22	0.20	2.20	2.35	0.33
	1045	1.053	0.36	1.20	0.23	2.23	2.27	0.36
	1145	1.010	0.36	1.23	0.27	2.27	1.74	0.74
	1245	1.025	0.40	1.19	0.32	2.32	1.86	0.82
	1345	1.100	0.38	1.22	0.29	2.29	1.71	1.03
	1503	1.339	0.41	1.19	0.33	2.33	2.00	1.07
	1545	1.565	0.35	1.25	0.33	2.33	2.30	1.01
	1630	1.991	0.36	1.23	0.24	2.24	2.03	2.17
	1700	2.471	0.37	1.20	0.27	2.27	--	--

$$\mu_o^{-1} = (\cosine \text{ solar zenith angle})^{-1}$$

$$\$ \frac{\tau(\lambda)}{\tau(\lambda_1)} = A \left(\frac{\lambda}{\lambda_1} \right)^{-\alpha}$$

(b) - The optical depth of dust on 6/6/77

Time	$\tau_{(0.45 \mu\text{m})}$	$\tau_{(0.55 \mu\text{m})}$	$\tau_{(0.65 \mu\text{m})}$	$\tau_{(0.84 \mu\text{m})}$	$\tau_{(1.04 \mu\text{m})}$
1100	0.84	1.05	1.30	0.94	0.93
1130	1.33	1.62	1.93	1.53	1.53
1200	2.30	2.60	2.99	2.58	2.58
1245	2.87	3.17	3.56	3.09	3.06
1330	2.22	-	2.89	2.50	2.62
1415	1.69	1.97	2.29	1.89	2.01
1505	1.02	1.23	1.46	1.16	1.23
1550	1.00	1.16	1.38	1.09	1.15
1630	0.90	1.04	1.22	0.97	1.03

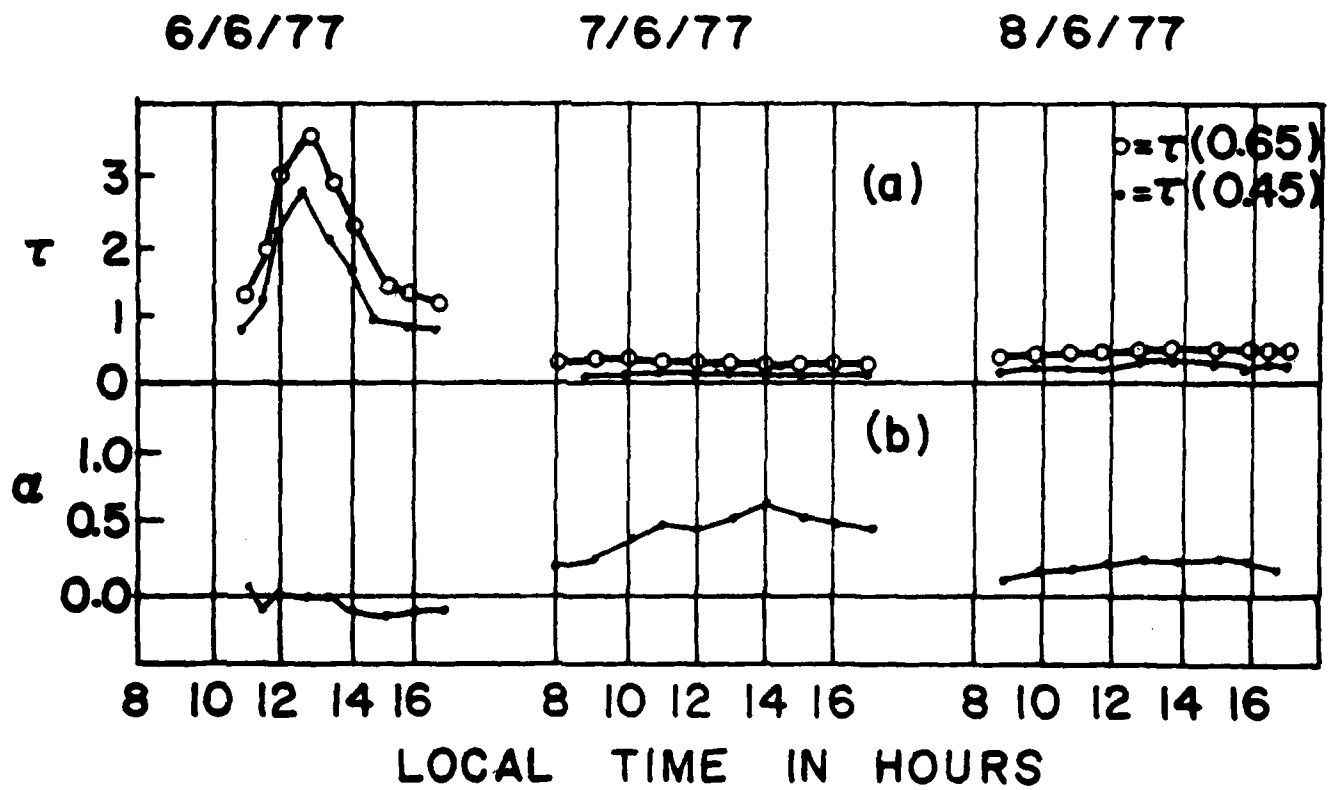


Fig. 21 The optical depths, $\tau(0.45 \mu\text{m})$ and $\tau(0.65 \mu\text{m})$ and the wavelength exponent α , versus time.

Returning to Fig. 20, we may compare parts a and b. It is clear that the optical depth, τ , is highly correlated to the total number of particles, N , as well as to the constant C of the power-law distribution fitted to the Royco data. The general shape of the curves is similar, although the details in the Royco data are not present in the optical depth.

The latter fact is even clearer in Fig. 20, and in Table 3 where we compared the exponent, β , of the power-laws derived from the in-situ Royco and from the optical data. The value of β_{optical} was calculated from the exponent of the wavelength dependence of the optical depth, α , (see Table 3) and is equal to

$$\beta_{\text{optical}} = 2 + \alpha$$

The average level of β_{optical} follows that of β_{Royco} on all three days including on June 8, when there occurred a weak dust storm. On the other hand, the optical method is unable to follow the fluctuations in β_{Royco} especially for large optical depths (6 June) or during the occurrence of dust increases (8 June). This is for several reasons. First, the optical measurement integrates over the whole atmosphere, whereas the Royco data are for the surface conditions only, where larger particles are more prevalent and fluctuation in the latter's amount more dominant. Secondly, the optical measurement integrates over all sizes between 0.1 and 1.0 to 2 μm . Thirdly, much of the fluctuations are in the large particle fraction ($r > 1 \mu\text{m}$) to which the optical method is relatively insensitive.

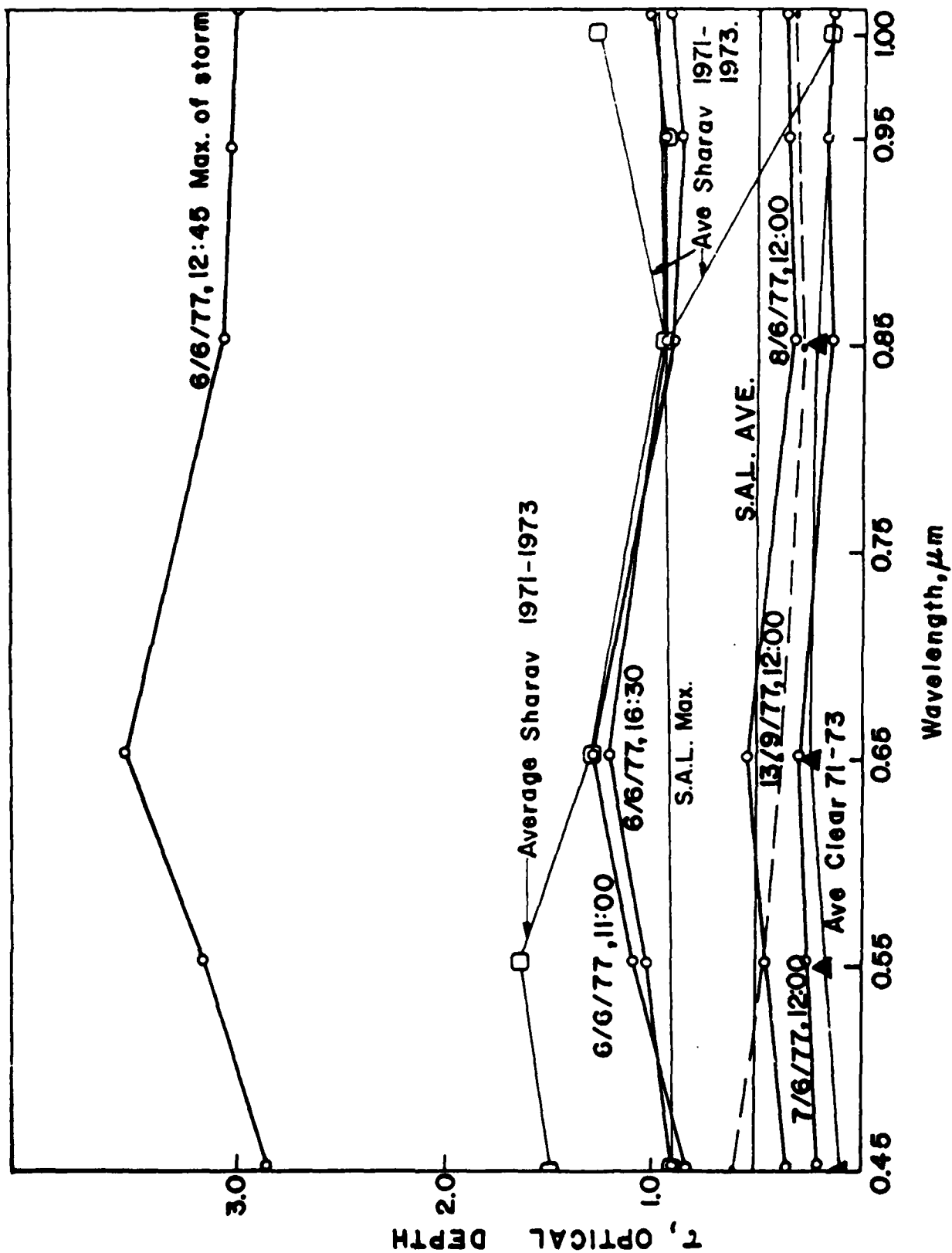
In Fig. 22, we compare some typical optical depths during the presently described dust storm with the average Sharav optical depths for the years 71-72 - a ratio of 3.1 is seen to occur - and with the average optical depths during cloud-free days in the years 1971-1973 - a ratio of 10:1 and larger occurs.

We furthermore compare with average and high optical depths of the Saharan aerosol layer over the Atlantic Ocean in summer (Carlson and Caverly, 1977), and with values for a cloud-free summer day, Sept. 13, 1977 in the high Negev Desert.

In all cases, the high optical depths occurring during the dust storm described in this paper are clearly brought out.

Such optical depths as observed during the dust storm usually occur for less than 10% of the year. However, slightly smaller optical depths of the order of 1,

Fig. 22 Typical curves of optical depth versus wavelength during the storm compared to data from other locations and from other times at Mitzpe Ramon, (S.A.L stands for Saharan Aerosol Layer).



sometimes leading to visibilities of less than 11 km at the surface occur in the Middle East about 150 days of the year (Lentz and Hoidale 1974) and are also common over the low-latitude Atlantic Ocean (Carlson and Caverley, 1977).

The whole range of optical depths we have just described is at least an order of magnitude larger than that of the Rayleigh atmosphere at the same wavelengths (0.36 - 0.01). Similarly, the dust optical depths during the Sharav are much larger than that of water-vapor or ozone in their absorption bands in the solar spectrum. The suitability of this storm for isolating the properties of the regional desert dust aerosol is thus obvious.

d. Summary and Conclusions.

The present study compares the properties of desert aerosol in the Middle East as measured by direct sampling and by spectral transmission of solar radiation. Such comparisons are of importance due to the need to extract as much information as possible from large scale remote sensing of aerosols in order to describe the latter's spatial and temporal variations for use in climate related studies as well as in the determination of long-range slant visibility and of sea-surface temperature from satellite data. The measured aerosol size distribution after the passage of the front was found to be similar to distributions measured by other investigators at other desert sites. This points to some commonality (Patterson and Gillette, 1977) in the desert aerosols around the world.

We have shown that the general time trends of the size distribution as measured in-situ are followed by the optical depth and its variation with wavelength. This may mean that the aerosol is often quite well mixed. On the other hand, detailed short-term fluctuations are not followed for the reasons mentioned in Section c.

We have observed that the simplest power law approximation poorly represents the size distribution of the aerosols during the peak of the dust storm. However, the fit to a power-law improves as the aerosol loading approaches that of normal weather conditions. A pure power-law size distribution is not usually found. During periods of low dust load, conditions are such that the average slope of the size distributions derived from optical measurements agrees with those from in-situ Royco observations.

It follows from our discussion that it will be difficult to ascertain the exact size distributions from remote optical observations at any given location. On the other hand, it also means that it is probably not important to resolve the exact size distribution with high resolution as to size and variability, at a given time in order to estimate the effects of an aerosol on the atmospheric energy balance. All aerosol size distributions with the same total number of particles, mean size and width will probably have the same optical effects (e.g. Hansen and Travis, 1974).

This will not be the case for the effect of the aerosol on cloud formation.

The imaginary part of the refractive index during the Sharav (Khamsin) period is lower by a factor of three to five than that during normal weather and quite similar to the values found in the U.S., Southwest and over the Atlantic Ocean. This shows again that desert aerosol is a distinct global type. Secondly, it shows that during normal weather situations, the contribution of the highly absorbing urban or organic aerosol to the imaginary part of the refractive index is important. Desert aerosol being composed primarily of siliceous clays, shows strong absorption bands in the 8-12 μm atmospheric window. (e.g. Fischer, 1976 Levin and Lindberg, 1979, Shipley et al, 1975 Grassl, 1973 Voltz 1973). The radiative effects of the desert aerosol are thus sensitively balanced between two opposing effects - the increase of Earth-Atmosphere albedo in the solar spectral range - leading to cooling of the affected layers and the underlying surface - and the increase of the greenhouse effect in the thermal IR - due to clogging of the 8-12 μm window.

The determination of any net climatic effects of the desert aerosol on regional or global scales is thus a delicate task and should be tackled by carefully planned studies - experimental programmes guided by sensitivity tests in atmospheric models.

Acknowledgements.

I would like to thank Mr. Baruch Starobinets and Mr. N. Sandlerman for their excellent aid in building and maintaining the equipment.

I would also like to thank J.D. Lindberg for his cooperation with the measurements and analysis of the first part of this report.

Thanks are also due to Professor J. Joseph and Dr. Yuri Mekler for their cooperation in the work and analysis of the second part of this report.

References

- Angstrom, A., 1929: On the atmospheric transmission of sun radiation and on dust in the air, Geogr. Ann., 11, 156; 12, 130.
- Angstrom, A., 1961: Techniques of determining the turbidity of the atmosphere, Tellus, 13, 214.
- Carlson, T.N., 1976: Large scale distribution of turbidity over the Northern Equatorial Atlantic. Proc. Symp. Radiation in the Atmosphere, Science Press, Ed. H.J. Bolle, 555.
- Carlson, T.N and R.S. Caverly, 1977; Radiative characteristics of Saharan dust at solar wavelengths. J. Geophys. Res., 82, 3141.
- Carlson, T.N., J.M. Prospero, 1972: Vertical and real distribution of Saharan dust over the Western Equatorial North Atlantic Ocean, J. Geophys. Res., 77, 5255.
- Chepil, W.S and N.P. Woodruff, 1963: The physics of wind erosion and its control. Advances in Agronomy, Vol. 15, Academic Press, 211.
- Deirmendjian, D, 1969: Electromagnetic scattering on spherical Poly-dispersions. Elsevier Press, pp 290.
- DeLuise, J.J., P.M. Furukawa, D.A. Gillette, B.G. Schuster, R.J. Charlson, W.M. Porch, R.W. Fegley, B.M. Herman, R.A. Rabinoff, J.T. Twitty and J.A. Weinman, 1976: Results of a comprehensive atmospheric aerosol-radiation experiment in the South-Western United States: Part I. Size distribution, extinction, optical depth and vertical profiles of aerosols suspended in the atmosphere, J. Appl. Met., 15, 441.

- DeLuise, J.J., P.M. Furukawa, D.A. Gillette, B.G. Schuster, R.J. Charlson, W.M. Porch, R.W. Fegley, B.M. Herman, R.A. Rabinoff, J.T. Twitty and J.A. Weinman, 1976: Results of a comprehensive atmospheric aerosol-radiation experiment in the South-Western United States: Part II. Radiation flux measurements and theoretical interpretation. J. Appl. Met. 15, 455.
- Fischer, K., 1976: The optical constants of atmospheric aerosol particles in the 7.5 - 1.2 μm spectral region. Tellus, 28, 266.
- Flohn, H., 1970: Etude des conditions climatiques de l'avance du desert. W.M.O Tech. Note.
- Gagin, A., 1971: Studies of the factors governing the colloidal stability of cumulus clouds. Proc. Inter. Weather Modif. Confer. Canberra, Australia, 5.
- Goldberg, E.D., 1971: Atmospheric dust - the sedimentary cycle and man. Comments on Earth Sciences, Geophys. 1, 117.
- Grassl, H., 1970: Determination of cloud drop size distribution from spectral transmission measurements. Contrib. to Atmos. Phys. 43, 255.
- Grassl, H., 1973: Separation of atmospheric absorbers in the 8 - 13 μm region. Cont., Atmos. Phys., 46, 75.
- Hanel, G., 1976: The properties of atmospheric aerosols as functions of the relative humidity at thermodynamic equilibrium with surrounding moist air. Advances in Geophysics, 19, Ed. by H.E. Landsberg and J. Van Miegham, Academic Press, 74.
- Hansen, J.E. and L.T. Travis, 1974: Light scattering in planetary atmospheres. Space Science Reviews, 16, 527.

- Joseph, J.H and A. Manes, 1971: Secular and seasonal variations of the atmospheric turbidity in Israel at Jerusalem, J. Appl. Met., 10, 453.
- Joseph, J.H., A. Manes and D. Ashbel. 1973: Desert aerosols transported by Khamsinic depressions and their climatic effects, J. Appl. Met., 12, 792.
- Joseph, J.H and N. Wolfson, 1975: The ratio of absorption to back-scatter of solar radiation during Khamsin conditions and effects on the radiation balance. J. Appl. Met. 14, 1389.
- Joseph, J.H., 1976: The effect of a desert aerosol on a model of the general circulation, Proc. Symp. Radiation in the Atmosphere, Science Press, Ed. H.-J. Bolle, 487.
- Joseph, J.H., 1977: Aerosol in a numerical model of the atmosphere, I.A.G.A - I.A.M.A.P Assembly, Seattle, Washington.
- Junge, C., 1963: Air chemistry and radioactivity, Academic Press.
- Junge, C., 1972: Our knowledge of physico-chemistry of aerosols in the undisturbed environment, J. Geophys. Res., 77, 5183.
- King, M.D., D.M. Byrne, B.M. Herman, J.A. Reagan. 1978: Aerosol size distributions obtained by inversion of spectral optical depth measurements. J. Atmos. Sci., 35, 2153.
- Kondratyev, K. Ya., O.D. Barteneva, L.I. Chapursky, A.P. Chernenko, V.S. Grishechkin, L.S. Ivlev, V.A. Ivanov, V.I. Korzov, V.B. Lipatov, 1973: "Aerosol in the GATE area and its radiative properties", Atmospheric Science Paper No. 247 Dept. of Atmos. Sci., C.S.U. pp. 109.
- Lentz, W.J and G.B. Hoidale, 1974: Estimates of the extinction of electromagnetic energy in the 8-12 μm range by natural atmospheric particulate matter. U.S. Army Electronics, E.C.O.M - 5228, Fort Monmouth, N.J.

- Levin, Z and J.Lindberg, 1979: Size distribution, chemical composition and optical properties of urban and desert aerosols in Israel. J. Geophys. Res., 84, 6941.
- Lindberg, J.D. 1975: Absorption coefficient of atmospheric dust and other strongly absorbing powders: An improvement on the method of measurements. Appl. Opt. 14, 2813.
- Lindberg, J.D, 1975: The composition and optical absorption coefficient of atmospheric particulate matter. Opt. and Quant. Electronics, 7, 131.
- Lindberg, J.D and L.S. Laude, 1974: A measurement of the absorption coefficient of atmospheric dust. Appl. Opt., 13, 1923.
- Lindberg, J.D., J.B. Gillespie and B.D. Hinds, 1976: Measurements of imaginary refractive indices of atmospheric particulate matter from a variety of geographic locations. Presented at the Inter. Symp. on Radiation in the Atmos., Garmisch-Partenkirchen, F.R.G. 19.
- Patterson, E.M. and D.A. Gillette, 1977: Commonalities in measured size distributions for aerosols having a soil derived component. J. Geophys. Res., 82, 2074.
- Patterson, E.M., D.A. Gillette and B.H. Stockton, 1977: Complex index of refraction between 300 and 100 nm for Saharan aerosols. J. Geophys. Res., 82, 3153.
- Petracca, C. and J.D. Lindberg, 1975: Installation and operation of an atmospheric particulate collector. U.S. Army Electronics Command Technical Report ECOM-5575, Fort Monmouth, N.J.
- Schutz, L., R. Jaenicke, 1974: Particle number and mass distributions above 10^{-4} cm radius in sand and aerosol of the Sahara Desert, J. Appl. Met. 13, 863.

Shipley, S., J.H. Joseph, J.T. Trauger, P.J. Guetter, E.W. Eloranta, J.E. Lawler, W.J. Wiscombe, A.P. Odell, F.L. Roester, J.A. Weinman, 1975: The evaluation of a shuttle-borne lidar experiment to measure the global distribution of aerosols and their effect on the atmospheric heat budget, Final Rept. NASA Grant NSG 1057, pp. 150.

SMIC, 1971: Inadvertent Climate Modification Report of Study of Man's Impact on Climate (S.M.I.C), MIT 201, pp. 308.

Twitty, J.T., R.J. Parent, J.A. Weinman, E.W. Eloranta, 1976: Aerosol size distributions: remote determination from airborne measurements of the solar aureole, Appl. Optics, 15, pp. 980.

Volz, F.E., 1973: Infra-red constants of ammonium sulfate, Sahara dust, volcanic pumice and flyash. Appl. Optics, 12, 564.